République Algérienne Démocratique et Populaire
Ministère de l'Enseignement Supérieur et de la Recherche Scientifique
Université Ibn Khaldoun de Tiaret
Faculté des Sciences Appliquées
Département de Génie Mécanique

MÉMOIRE DE FIN D'ETUDES

Pour l'obtention du Diplôme de Master

Domaine : Sciences et Technologie
Filière : Génie Mécanique
Parcours : Master
Spécialité : Énergétique

Thème

New design of a porous aerostatic bearing with variable permeability

Préparé par :
AZZEDINE Omar El Farouk
CHEKIRINE Mohamed Badredine

Soutenu publiquement le : 20 / 06 / 2024, devant le jury composé de :

Mr. DEBBIH Senouci	Maître de Conférences "A" (Univ. Ibn Khaldoun)	Président
Mr. KARAS Abdelkader	Professeur (Univ. Ibn Khaldoun)	Examinateur
Mr. BENARIBA Aboubakeur	Maître de Conférences "A" (Univ. Ibn Khaldoun)	Examinateur
Mr. ABOSHIGHIBA Hicham	Maître de Conférences "B" (Univ. Ibn Khaldoun)	Encadrant

Année universitaire : 2023 - 2024

People's Democratic Republic of Algeria
Ministry of Higher Education and Scientific Research
Ibn Khaldoun University of Tiaret
Faculty of Applied Sciences
Department of Mechanical Engineering

GRADUATION THESIS

For the Award of the Master's Degree

Field : Sciences and Technology
Department : Mechanical engineering
Program: Master's
Specialty : Energetic

Topic

New design of a porous aerostatic bearing with variable permeability

Prepared by :
AZZEDINE Omar El Farouk
CHEKIRINE Mohamed Badredine

Publicly defended on: : 20 / 06 / 2024, in front of the jury composed of :

Mr. DEBBIH Senouci	Senior lecturer "A" (Univ. Ibn Khaldoun)	President
Mr. KARAS Abdelkader	Professor (Univ. Ibn Khaldoun)	Examiner
Mr. BENARIBA Aboubakeur	Senior lecturer "A" (Univ. Ibn Khaldoun)	Examiner
Mr. ABOSHIGHIBA Hicham	Senior lecturer "B" (Univ. Ibn Khaldoun)	Supervisor

Academic year : 2023 - 2024


بسم الله الرحمن الرحيم

Acknowledgments

First and foremost, we thank **ALLAH**, who gave us the strength and courage to elaborate this thesis.

We extend our heartfelt appreciation to our advisor, Mr. Hicham ABOSHIGHIBA, for his unwavering guidance and encouragement throughout this journey.

Our sincere thanks go to Pr. DEBBIH Senouci, Senior lecturer at the Department of Mechanical Engineering for having accepted to chair the jury,
And esteemed members of the jury :
Pr. KARAS Abdelkader, Professor at the Department of Mechanical Engineering,
Dr. BENARIBA Aboubaker, Senior lecturer at the Department of Mechanical Engineering, for accepting to evaluate our thesis.

We want to express our sincere thanks to all the teachers of the departement of Mechanical Engineering.

Finally, and most importantly, our deepest gratitude goes to our parents. Their unwavering support, blessings, and encouragement throughout our studies and this entire thesis process have been invaluable. Words cannot express how much we appreciate everything they have done for us. We extend our love and gratitude to our families for their constant support, which have shaped us into who we are today.

With immense gratitude, we dedicate this work to:

Our dear parents,

This achievement wouldn't have been possible without you.

We want to express our deepest gratitude for the countless sacrifices you've made for us since we were born.

Thank you for the unwavering love and constant support that you've showed us throughout our lives. Your encouragement and prayers, especially during our academic journey, mean the world to us.

Words seem inadequate to express our immense thanks and appreciation.

To our cherished family members,

To our fellow students and study buddies,

To our dedicated teachers,

To all those who hold a special place in our hearts.

CONTENTS

List of Figures

List of Tables

Nomenclature

SYMBOL	UNIT	SIGNIFICATION
M	$[Kg]$	Rotor mass
s		Rigidity of shaft
e		Eccentricity of rotor
y		Additional rotor deviation
D_v	$\left[\mathrm{m}^3/\mathrm{s}\right]$	The volimic flow
D	$[m]$	diameter of the cylinder
h	$[\mu m]$	thickness of thin film
W	$[N]$	force of lift
A	$\left[\mathrm{m}^2\right]$	Surface
L	$[m]$	Length
P	[Pa]	Pressure
R	$[m]$	cylinder radius
t	$[s]$	Time
U,V,W	$\left[m \cdot s^{-1}\right]$	Axial, radial and circumferential speed

GREECE SYMBOLS

∇		gradient operator
ω	$[\mathrm{rad/s}]$	angular speed of the shaft
δ		Static deformation of the shaft
μ	$[\mathrm{Kg/m.s}]$	Dynamic viscosity
ν	$\left[m^{-2} \cdot s^{-2}\right]$	kinematic viscosity
Δ		difference operator
∂		partial derivative
ρ		Fluid density

DIMENSIONLESS NUMBERS

k	Permeability
Re	number of Reynolds
Re_k	Reynolds number based on permiability
f_k	friction factor

GENERAL INTRODUCTION

GENERAL INTRODUCTION

In a rotating machinery setup, bearings serve as mechanical aids responsible for guiding shafts and managing vibrations. They are available in different types such as rolling-contact, hydrodynamic, and electromagnetic varieties. Among these, hydrostatic bearings, a type of hydrodynamic bearing, provide a beneficial method for controlling rotor vibrations. Aerostatic bearings offer another approach within fluid film bearings, utilizing an open-loop fluid system where air, after filtration, is injected into the bearing clearance and then released into the surrounding environment.

This project focuses on investigating how the permeability of aerostatic bearings affects the dynamic response of the rotors they support.

Our investigation leverages a 3D computational fluid dynamics (CFD) using Ansys-CFX software. Initially, the model undergoes validation against established experimental data from the relevant literature. Subsequently, we will incorporate design modifications to explore the relationships between bearing parameters and rotor vibration. This analysis aims to identify potential design principles for new vibration control methods.

The present thesis is structured in three chapters and is organized as follows :

CHAPTER 1 A bibliographical research on bearings in general and porous media is presented.

CHAPTER 2 Delves into the governing mathematical equations that describe the behavior of porous media bearings and their associated characteristics.

CHAPTER 3 Model validation is achieved by contrasting the numerically generated results with corresponding experimental data obtained from relevant articles.

The culmination of this research effort involves the formulation of conclusions based on the acquired data. and suggesting avenues for further exploration to drive progress in this field.

CHAPTER I

BIBLIOGRAPHICAL RESEARCH

Chapter I

BIBLIOGRAPHICAL RESEARCH

I.1 Introduction

The main purpose of this chapter is to present a research bibliography on three key areas relevant to machine dynamics: rotor dynamics, bearings, and porous media. Rotor dynamics focuses on the classification of rotors by type and explores vibration control methods, encompassing both passive and active techniques. Bearings delve into various types and offer a detailed examination of hydrostatic bearings. Finally, porous media cover classification and explore their properties.

I.2 Rotors

In the realm of mechanics, It's the ever-churning center that pulls everything in and sets it spinning. It can be a physical component like the ones found in engines or turbines, but the concept extends beyond the machine world.

I.2.1 Rotor dynamic Behavior

Rotor dynamic is the study of the stability of rotating machinery. It involves analyzing the dynamic behavior of rotors, including their vibrations, stresses, and deflections. As the rotational speed of a rotor increases, its vibration levels often pass through a critical threshold known as

the critical speed. This vibration is typically caused by rotor imbalance, and if the vibration amplitude at these speeds becomes excessive, catastrophic failure can occur. Rotor dynamic analysis can help to identify and mitigate these risks by predicting the behavior of rotors under various operating conditions. This information can be used to design rotors that are more stable and reliable, and to avoid operating conditions that could lead to failure.

I.2.2 Composition of the rotor shaft system

These rotating components are generally made up of several parts designed to work together to perform a specific function. Here are some of the essential components of a rotor [1] :

- **Shaft**: The main structural component that supports the rest of the rotor and rotates around its axis.
- **Discs**: Rotating components responsible for converting energy into motion or force. They can take different forms, such as blades, spirals, or vanes, depending on the application.
- **Hub**: Structure that attaches to the shaft and supports the rotor blades, ensuring stability and structure.
- **Casing**: This outer structure protects the rotor and supports the internal elements. It may include specialized passages to direct the flow of fluids or gases.
- **Bearings**: Components that allow the rotor to rotate smoothly and with minimal friction.
- **Seals**: Components that prevent leaks and ensure that fluids or gases are contained in the system.

Other components can include cooling systems, damping mechanisms, and fluid passages, as well as other specialized components specific to the application of the particular rotor.

Additional Information: The specific components of a rotor will vary depending on its application. For example, a helicopter rotor will have different components than a wind turbine rotor.

The materials used to make rotors will also vary depending on the application. For example, a

rotor that is used in a high-temperature environment will need to be made from a material that can withstand the heat. The design of a rotor is critical to its performance. Factors such as the shape of the blades, the angle of attack, and the rotational speed all affect the rotor's efficiency and power output.

I.3 Rotor Shaft Types

The selection of a rotor shaft significantly impacts a machine's rotor dynamic behavior. Here's a breakdown of two common types:

I.3.1 Flexible Rotor Shafts

Flexible shafts exhibit a greater capacity to bend or flex when placed under load. Compared to their rigid counterparts, they possess lower stiffness. This flexibility makes them well-suited for applications where a degree of misalignment between connected components is likely; they can better tolerate this misalignment. Additionally, flexible shafts become necessary when the operating speeds must exceed the system's critical speeds. Careful balancing, along with the flexible shaft's characteristics, is crucial for smooth operation in these scenarios. Examples of flexible shaft applications include dental drills (where they manage high speed and small alignment shifts), driveshafts in certain vehicles, and power transmission systems within complex machinery.

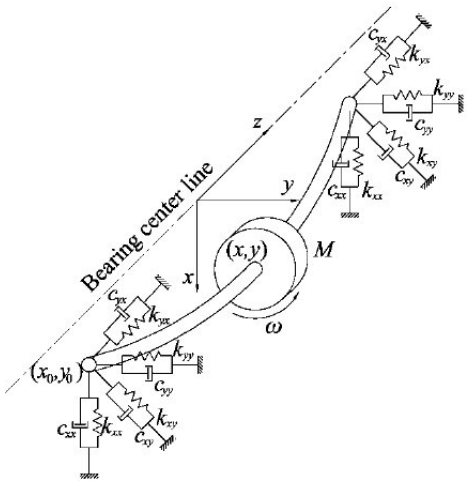

Figure I.1: Flexible rotor system [2]

I.3.2 Rigid Rotor Shafts

Rigid shafts are designed to experience minimal deflection or bending under standard operating loads. Their primary function is to maintain their shape even during high-speed rotation. This property makes them ideal for applications where the rotor's operating speed remains consistently below the critical speed. Operating within these parameters helps prevent excessive vibration that could potentially compromise the system. You'll often find rigid shafts used in lower-speed machinery, simple rotating systems, and various power tools.

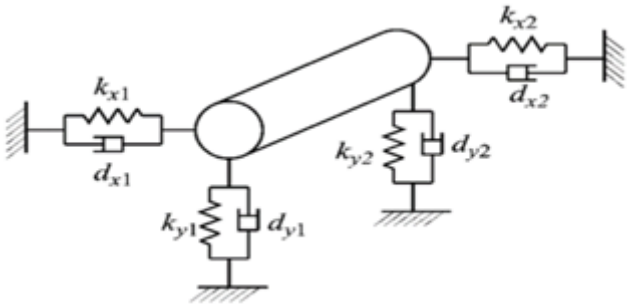

Figure I.2: Rigid rotor system [3]

The choice of the appropriate rotor shaft type depends on several factors, including:

Operational Speed: High-speed applications necessitate flexible shafts for vibration dampening, while lower-speed applications can utilize rigid shafts for their robustness.

Power Transmission Requirements: The shaft must be able to handle the transmitted power without excessive deflection.

Precision Needs: High-precision applications may require stiffer shafts with tighter tolerances.

I.4 Rotor vibration control

I.4.1 Passive Vibration Control

Passive vibration control systems address vibrations without the need for external power or sophisticated control systems. They work by dissipating or absorbing vibrational energy through their design features or using added components. These systems are known for their simplicity, reliability, and cost-effectiveness. Examples of passive techniques include balancing weights,

viscous dampers, squeeze film dampers, and tuned mass dampers. While effective, their performance is fixed, and they might not be ideal for handling widely fluctuating vibration conditions.[4]

I.4.2 Active Vibration Control

Active vibration control employs a more complex approach. These systems use sensors to continuously monitor vibrations and actuators to apply calculated, counteracting forces. Sophisticated control algorithms help the system adapt to changing conditions. This adaptability leads to superior vibration reduction and can even allow for lighter, more flexible rotor designs. However, active systems come with increased complexity, higher cost, and require sensors, control systems, and a power source.[4]

I.4.3 When to Choose Which

Passive systems excel when simplicity, reliability, and predictable vibration sources are paramount. Active control is the ideal choice when adaptable, high-performance vibration suppression is a necessity, or if the rotor design needs maximum flexibility. Many real-world systems combine aspects of both active and passive control to optimize vibration reduction while balancing cost and complexity.

I.5 Bearings

In the domain of mechanical engineering, bearings serve as critical components within a multitude of machines, devices, and systems. Their primary function is to provide support for the loads experienced by moving parts while minimizing frictional losses at the contact interface. By enabling precise rotational alignment and mitigating wear and tear, bearings enhance the operational efficiency and reliability of these mechanisms.

There are several types of bearing, each designed to meet requirements specific application. Common types include ball bearings, roller bearings, plain bearings (hydrodynamic and hydrostatic bearings) and thrust bearings.

I.5.1 Applications of bearings

In general machinery, bearings are found in rotating components such as shafts, axles, and gears. They enable smooth rotation and reduce wear. They are also found in linear motion systems, such as drawer slides and printer carriages.

In transportation, bearings are present in wheels, steering systems, engines, and gearboxes of vehicles. Heavy machinery, such as construction equipment and industrial robots, use bearings to support heavy loads and ensure precise movement. In high-precision applications, such as medical and scientific instruments, bearings enable precise and frictionless movement.

Their importance is often overlooked, but they contribute significantly to the performance and longevity of mechanical systems.

I.5.2 Type of bearing

Ball bearings

In machines, bearings function as friction-reducing interfaces for rotating parts. They comprise two rings with rolling elements, such as balls, rollers, or needles, positioned between them.

Figure I.3: Ball bearing [5]

Hydrodynamic bearings

Hydrodynamic bearings rely on a thin layer of oil or water (the lubricant film) to separate and lubricate the contacting surfaces. This film is generated by the shaft's rotation, which wedges the lubricant into the narrowing space between the bearing and the shaft.

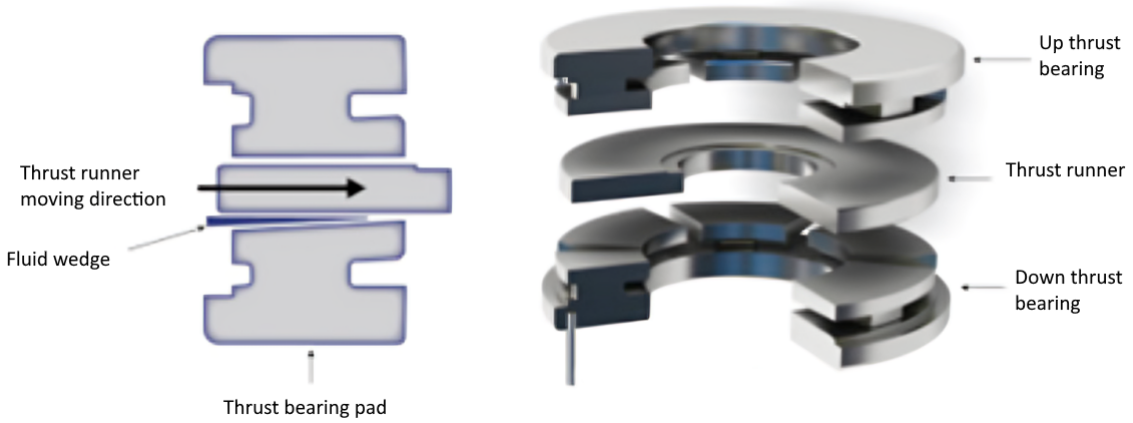

Figure I.4: Parts of hydrodynamic bearing [6]

Hydrostatic Bearing

Unlike hydrodynamic bearings, hydrostatic bearings utilize an external pump to generate a pressurized film of air or oil. This pressurized film separates and lubricates the contacting surfaces.

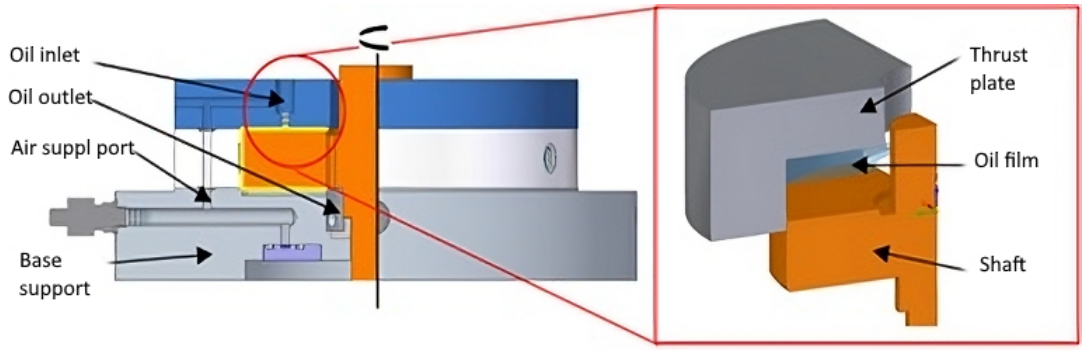

Figure I.5: Components of hydrostatic bearing [3]

I.6 Hydrostatic Bearing

I.6.1 Lubrication and mechanism of action

Hydrostatic bearings achieve friction reduction through a pressurized oil or air film separating the contacting surfaces. This film is generated by an external pump forcing fluid into designated ports on the bearing. The pressurized fluid then flows between the surfaces, creating a lubricating layer that minimizes friction and wear.

And we have two main methods used to introduce the fluid inside the hydrostatic bearings are:

- Constant flow supply, this type of lubrication is only valid for liquids.
- Constant pressure supply.

In constant flow systems, a constant flow pump is placed between the reservoir and the alveolus (Figure 1.6). When the mechanism has several alveoli, it is possible to either supply each stop with an individual pump or to use constant flow regulators to distribute the fluid from a single pump. This solution, which ensures great rigidity, is little used because it is complex and expensive. Constant pressure systems are preferred.[7]

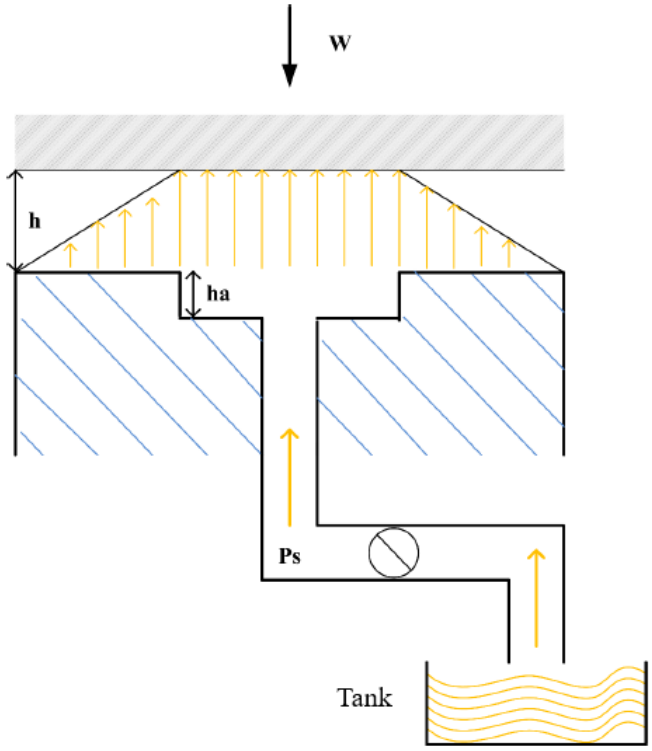

Figure I.6: Constant flow supply [7]

In constant pressure mechanisms, a hydraulic resistance is placed immediately upstream of the recess (Figure 1.7). The most frequently used types of resistances are capillary tubes and thin-walled orifices (diaphragms). Sometimes nozzles are used, which represent a compromise between the two previous systems. Self-regulating resistances (of the servo valve type) are also used, which have a variable resistance with the flow rate, this allows the stiffness of the plateau to be increased. Theoretically, it is possible to design variable resistances such that the stiffness of the mechanism is infinite, in practice, these variable resistances are sometimes sources of self-sustained oscillations: the plateau then becomes a vibration generator.[7]

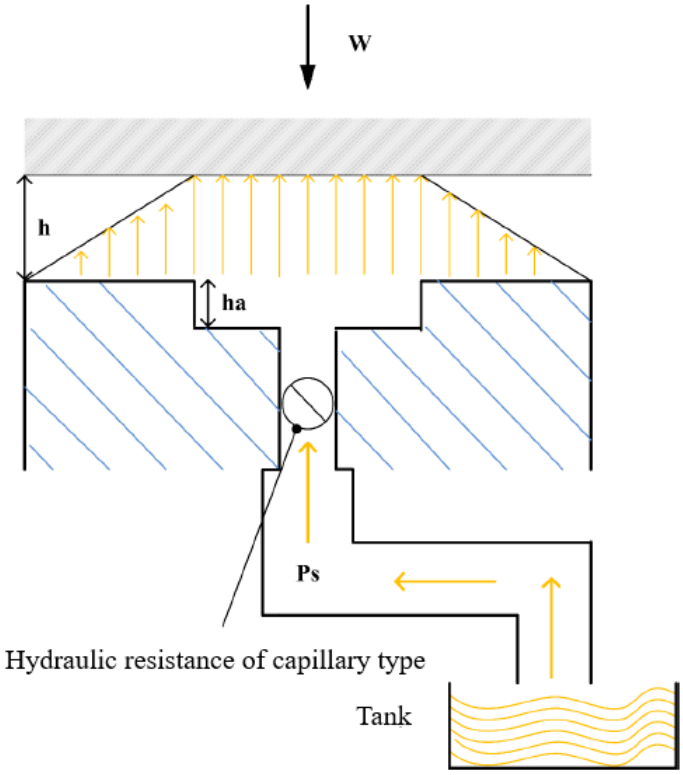

Figure I.7: Constant pressure supply [7]

I.6.2 Creation of the Hydrostatic fluid film

The formation of a fluid film in a hydrostatic thrust bearing is shown in Figure 1.9.

- (a): The pump is off.
- (b): The pressurized fluid begins to flow to the thrust bearing and the pressure in the pocket increases.
- (c): The pocket pressure increases until the pressure across the pocket surface is sufficient to lift the applied load.
- (d): The bearing starts to operate, the fluid flows through the system, and a pressure drop exists between the pressure source and the pad, and between the pocket and the pad outlet.
- (e): As the load increases, the film thickness decreases and the pocket pressure increases until the integrated pressure across the bearings is equal to the applied load.
- (f): When the load decreases, the film thickness increases and the pocket pressure decreases.

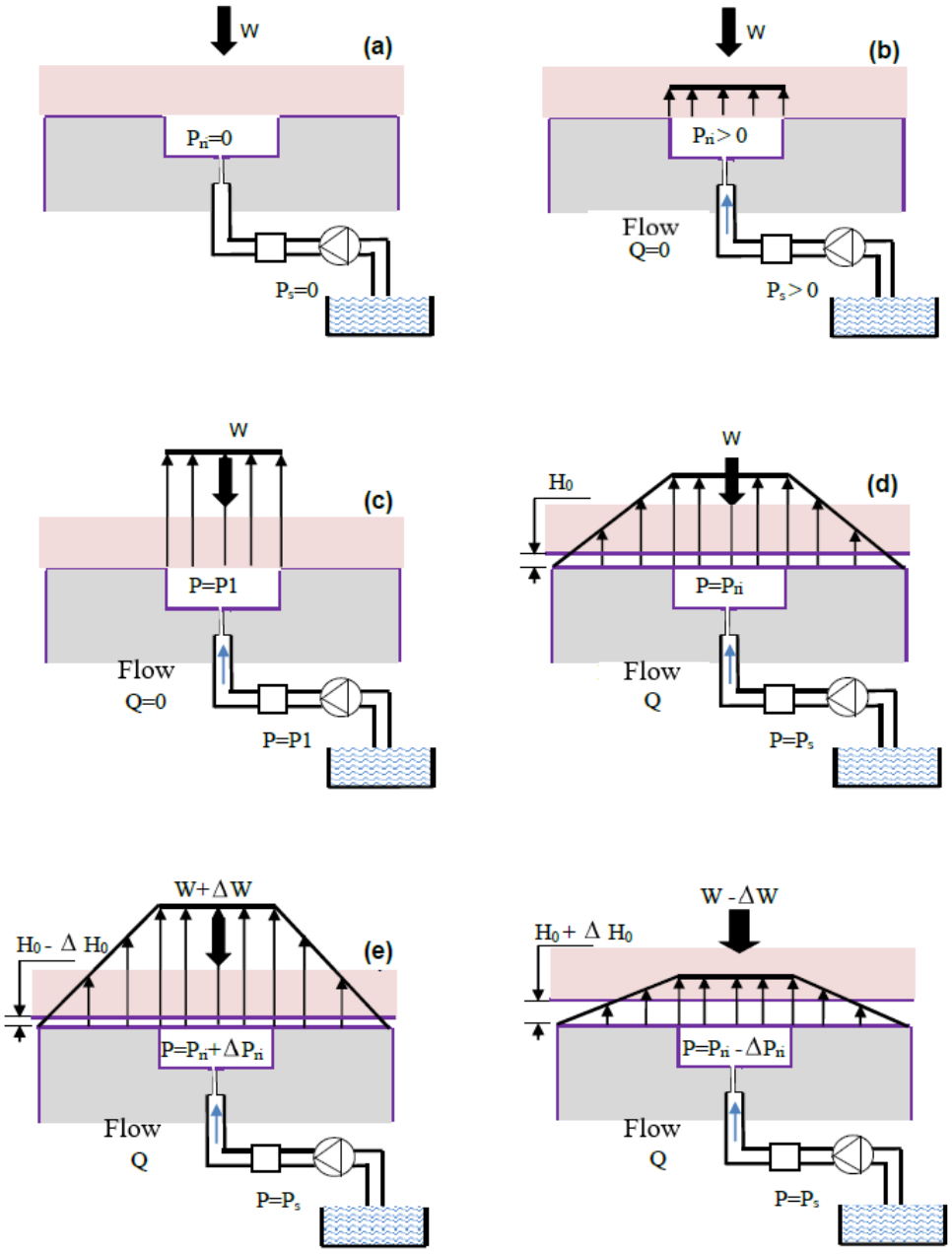

Figure I.8: Creation of fluid film in hydraustatic bearing [7]

I.6.3 Types of Hydrostatic Bearings

Orifice Bearings

Orifice bearings are the simplest and most common type of hydrostatic bearing. They use orifices to generate pressurized fluid films. The fluid is injected under pressure into the orifices, then flows between the contacting surfaces, creating a separating layer that reduces friction and wear.

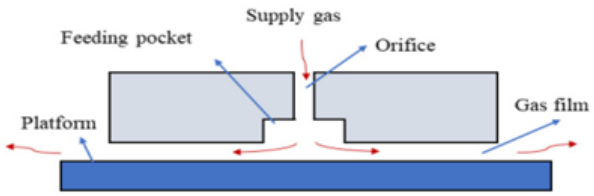

Figure I.9: Schematization of orifice bearing [8]

Capillary Bearings

Capillary bearings use capillaries to generate pressurized fluid films. The fluid is drawn into the capillaries by capillary action, then flows between the contacting surfaces, creating a separating layer that reduces friction and wear.[9]

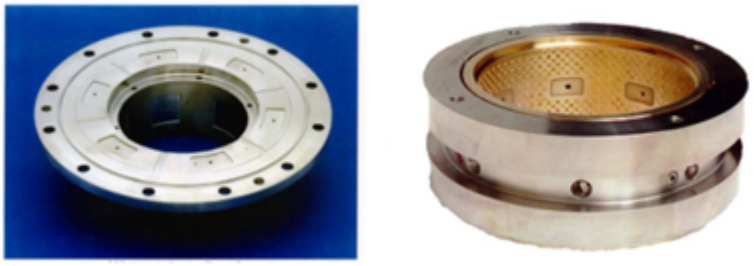

Figure I.10: Example of capillary bearing [9]

Porous Bearings

Porous bearings use a porous material to generate the pressurized fluid film. The fluid is injected under pressure into the porous material, then flows between the contacting surfaces, creating a separating layer that reduces friction and wear.

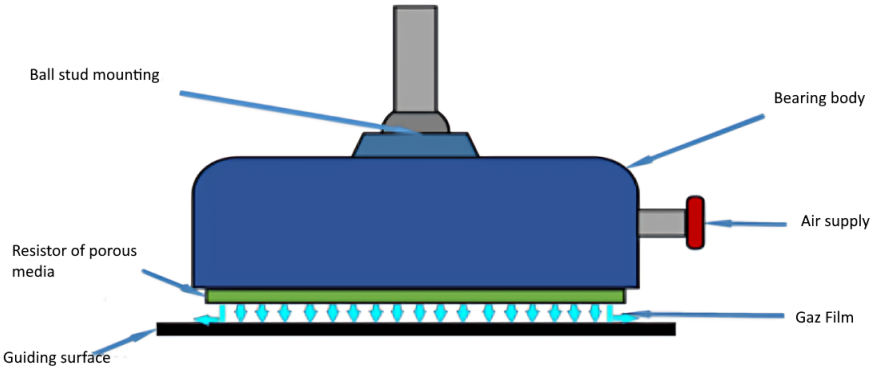

Figure I.11: Principle of porous air bearing [10]

I.7 Porous Media

A porous medium is typically defined as a solid matrix containing interconnected or isolated void spaces. Put another way, it's a solid material with a significant volume of pores, either neatly arranged or distributed randomly, that can be interconnected or separate, as shown in Figure I.12. These void spaces, known as porosity, exhibit a wide range of shapes and sizes.

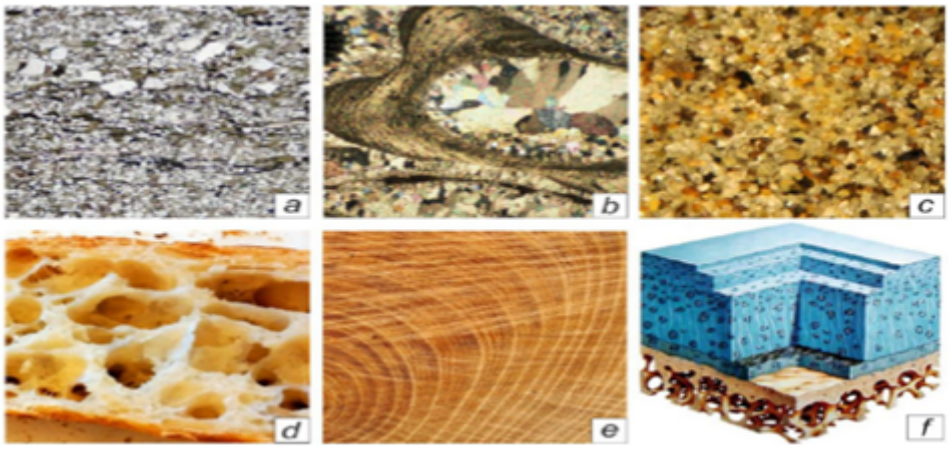

Figure I.12: Examples of natural porous materials
a) sandstone, b) limestone, c) beach sand, d) bread, e) wood, f) articular cartilage. [11]

I.7.1 Classification of porous media

The classification of porous media can be established based on the structure of the solid material that forms the matrix (Figure I.12). Here, we'll explore three distinct categories:

Granular Media

A granular medium is comprised of a multitude of separate solid particles, known as grains, that lack chemical bonding between them. Examples of granular media include sand, gravel. These materials are characterized by [11]:

- **Intergranular porosity**: The void spaces between the individual grains contribute to the overall porosity.
- **High permeability**: Due to the interconnected nature of the pores, fluids can readily flow through the medium.

- **Low specific surface area**: The total surface area of the solid material per unit volume is relatively small compared to other types of porous media.

Cellular Media

In cellular media, the solid component forms distinct cells, which can be either open or closed. Examples include foam, bone, and certain types of ceramics. These materials exhibit the following characteristics [11]:

- **Cellular porosity**: The porosity arises from the presence of these internal cells within the solid structure.
- **Variable permeability**: The permeability can vary depending on the size, shape, and connectivity of the cells.
- **Moderate specific surface area**: Compared to granular media, cellular media offers a higher specific surface area due to the internal cell walls.

Fibrous Media

The solid portion of a fibrous medium consists of interwoven fibers that are often bound together by a binder. Paper, felt, and textiles are all examples of fibrous media. These materials are characterized by [11]:

- **Inter-fiber porosity**: The void spaces between the entangled fibers contribute to the overall porosity.
- **Anisotropic permeability**: The permeability can be directionally dependent, meaning it may vary depending on the flow direction relative to the fiber alignment.
- **High specific surface area**: Due to the high surface-to-volume ratio of the fibers, fibrous media generally possess a high specific surface area.

I.7.2 Properties of Porous Media

Porous media are characterized by a complex structure consisting of a solid matrix and interconnected void spaces called pores. These materials exhibit a variety of properties that are crucial for understanding their behavior and performance in various applications.[12]
Here, we delve into some key properties of porous media:

Porosity

Defined as the ratio of pore volume to the total volume of the material, porosity is typically expressed as a percentage. It signifies the storage capacity of a porous medium and can be classified into different types, such as open and closed porosity.

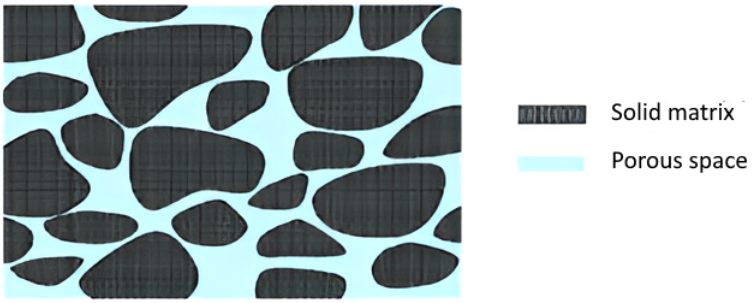

Figure I.13: Empty space in a porous media [13]

Permeability

A measure of the ability of a fluid to flow through a porous medium, permeability is usually expressed in Darcy (D) units. It is highly influenced by the pore size and connectivity, with higher permeability indicating easier fluid flow.

Tortuosity

Quantifies the deviation of the fluid flow path from a straight line within the pores. Having a value equal to or greater than 1, tortuosity represents the increased resistance encountered by the fluid due to the winding path. we can determine the tortuosity as :

$$\tau = \frac{Le}{L}$$

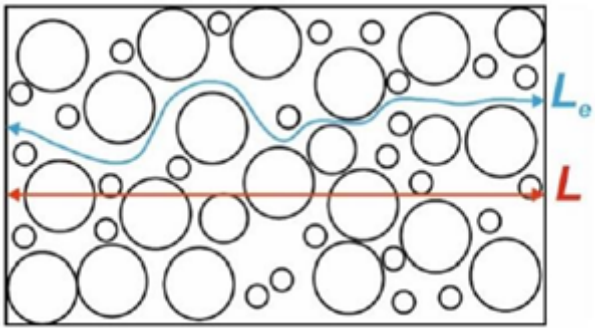

Figure I.14: Notion of tortuosity of a porous medium [14]

Specific Surface Area

Represents the total surface area of the solid accessible to the fluid per unit volume of the material. It plays a vital role in processes like chemical reactions and adsorption, with higher specific surface area enhancing the interaction between the fluid and the solid.

Compressibility

The ability of a porous medium to deform under an applied pressure or is the property of material that describes the change relative volume dV/V (or deformation) to the initial volume V when subjected to a change in stress under isothermal conditions.

Electrical Conductivity

Certain porous media, including rocks and soils, exhibit electrical conductivity. This phenomenon arises from the presence of conductive minerals within the solid matrix or electrolyte-filled pores. Electrical conductivity measurements serve as a valuable tool for both characterizing these materials and delineating the spatial distribution of subsurface fluids and mineral deposits.

I.8 Flow in porous media

The investigation of flow phenomena within porous media necessitates the application of diverse models that incorporate fundamental laws governing mass transport, energy transfer, and momentum. This field finds application in various domains such as hydrology, petroleum engineering, and filtration. It involves the movement of a fluid (liquid or gas) through a solid material with interconnected pores. The structure and properties of the porous medium, as well as the characteristics of the fluid, greatly influence this flow.

The permeability of the material, defined as its ability to allow fluid passage, plays a central role. Porosity, indicating the fraction of void space in the material, is also important. The viscosity of the fluid and the applied pressure also influence the flow.

Several laws and models describe fluid flow in porous media. Darcy's Law is fundamental for low-velocity flows. It states that the flow rate is proportional to the permeability, the pressure gradient, and the inverse of the viscosity.

Other more complex laws and models, such as the Navier-Stokes equation and the Richards equation, consider non-linear effects and unsaturated flow.

CHAPTER II

MATHEMATICAL FORMULATION

Chapter II

MATHEMATICAL FORMULATION

II.1 Introduction

This chapter explores the essential mathematical models used to analyze air bearings. Air bearings, employing a thin layer of compressed air for load support and friction reduction, rely on these models to determine key parameters like pressure distribution and lift force. Understanding these models is critical for evaluating the performance and stability of air bearings in various applications.

II.2 Physical properties of porous materials and fluid

II.2.1 Porosity

Porosity (φ) is a quantitative measure of the void fraction within a porous medium. It is defined as the ratio of the pore volume (Vp) to the total volume (VT) of the material. Porosity is a dimensionless quantity typically expressed as a decimal or a percentage.

The porosity of a material significantly impacts its physical properties. For instance, porous media generally exhibit lower bulk density compared to non-porous materials. Additionally, they often demonstrate enhanced resilience and higher permeability (K), which signifies their ability to facilitate fluid flow through their interconnected pore network.

$$\varphi = \frac{Vp}{V_T} \tag{II.1}$$

φ: porosity,

Vp : the pore volume,

Vt : the total volume of the material.

II.2.2 Permeability

Permeability(K) is a quantitative descriptor of a porous medium's capacity to facilitate fluid flow through its interconnected pore network. It's defined as the proportionality constant relating the specific discharge of a viscous, incompressible fluid to the applied pressure gradient(ΔP).
Permeability is typically expressed in units of square meters per second (m^2/s).
Darcy's law is a physical principle that describes the flow of an incompressible and viscous fluid through a porous medium. It is expressed by the following equation:

$$\frac{\Delta \mathrm{P}}{\Delta \mathrm{x}} = \frac{\mu}{k} v \tag{II.2}$$

Darcy's law, while a fundamental principle for describing fluid flow in porous media, is a simplified model that does not account for all influencing factors. It assumes laminar flow of an incompressible, Newtonian fluid, neglecting the effects of turbulence and fluid Compressibility. Despite these limitations, Darcy's law remains a valuable tool for understanding and predicting fluid flow in porous media.

II.2.3 Forchheimer law

The pressure-to-momentum flux ratio within the porous media $\frac{\Delta \mathrm{P}}{\Delta \mathrm{x}}$ is governed by a combination of inertial and viscous contributions. Darcy's law captures the viscous contribution, relating it directly to the pressure gradient and inversely to the fluid viscosity. However, at higher velocities, inertial effects become significant, rendering Darcy's law inapplicable. Forchheimer's law incorporates these inertial effects by introducing a term proportional to the square of the pore

fluid velocity.

$$\frac{\Delta P}{\Delta x} = \frac{\mu v}{k} + C\frac{\rho v^2}{k^{1/2}} \tag{II.3}$$

The Forchheimer inertia coefficient (C), a dimensionless parameter, is employed to quantify inertial effects within porous media. The previously derived equation allows for the determination of C based on the known permeability (k) and a specified pressure difference (ΔP). By adopting the square root of permeability ($k^{1/2}$) as the characteristic length scale of the porous media, the following definition for the permeability-based Reynolds number (Re_k) can be established:

$$Re_k = \frac{\rho v^2 k^{1/2}}{\mu} \tag{II.4}$$

By defining the dimensionless friction factor f_k as follows:

$$f_k = \frac{\Delta P}{\Delta x}\frac{k^{1/2}}{\rho v^2} \tag{II.5}$$

And by substituting (II.4) and (II.3) in the expression (II.5) one obtains:

$$C = f_k - \frac{1}{\mathrm{Re}_k} \tag{II.6}$$

In equation (II.5) for a relatively small Reynolds number we will consider that Coefficient of inertia is negligible.

II.2.4 Density

Density To quantify the mass of fluid transferred during the flow, one must know the amount of mass contained in a unit volume of fluid, that is, its density. The density ρ of a material represents the amount of mass M that the material contains per unit volume V.

$$\rho = \frac{M}{V} \tag{II.7}$$

II.2.5 Viscosity

Fluids naturally resist flow when different layers try to move at different speeds. This resistance is like friction between the layers, and it's what we call viscosity. Basically, all fluids have some level of viscosity, which makes it harder for them to flow smoothly.

There are two common viscosity measurements, dynamic viscosity μ and kinematic viscosity v.

The relationship between dynamic viscosity and kinematic viscosity is shown below:

$$v = \frac{\mu}{\rho} \tag{II.8}$$

v : Kinematic Viscosity

μ : Dynamic Viscosity

ρ : Density

II.3 Dynamic characteristics

A linear study is conducted under the assumption that the journal is perfectly rigid and restricted to small displacements around a static equilibrium position. This involves two steps [7]:

- **Static Analysis:** Determine the static equilibrium position of the journal within the bearing under an external load.
- **Linearized Dynamic Analysis:** Analyze the linearized dynamic motion of the rotating journal (shaft) around the static equilibrium position O.

This linear analysis of the bearing's behavior around the static equilibrium position allows for the modeling of the lubricant film using stiffness and damping coefficients (Figure II.1).

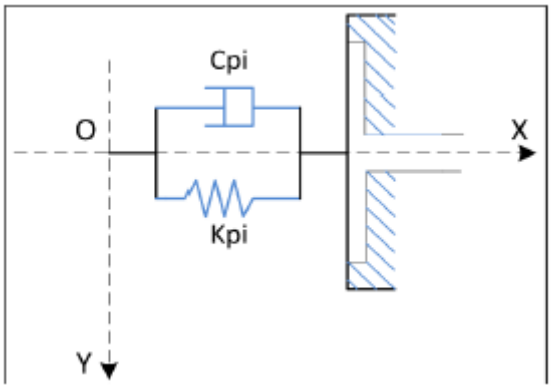

Figure II.1: Schematic representation of stiffness and damping for a hydrostatic thrust bearing [7]

Determining the stiffness and damping coefficients of the lubricant film in a journal bearing has several important applications:

1. **Assessing Stability:** These coefficients are crucial for evaluating the stability of an operating point, particularly in determining the critical mass of the rotating journal. The critical mass is the maximum mass that the bearing can support without experiencing instability.

2. **Modeling Fluid Film Effects:** The coefficients allow for incorporating the influence of the fluid film on the dynamic response of a structure, such as a shaft subjected to low-amplitude dynamic excitations. By considering these coefficients, engineers can accurately predict the shaft's behavior under various dynamic loads.

3. **Identifying Critical Shaft Speeds:** The stiffness and damping coefficients play a vital role in identifying the critical speeds of the shaft. Critical speeds are rotational speeds at which the shaft's natural frequencies coincide with the excitation frequencies, leading to resonant vibrations and potential instability. Determining these critical speeds is essential for safe and reliable operation of rotating machinery.

II.3.1 Dynamic coefficients of a single-acting hydrostatic thrust bearing

The calculation of dynamic coefficients is done by a method called small displacements and small velocities. If a small displacement x_i and a small displacement velocity $\dot{x}_i$ are imposed in the vicinity of the static equilibrium position (x_0, y_0) collinear with the axis (o,x) we can write [7] :

$$W_{pi}(x_0 + x_i, y_0, \dot{x}_i, \dot{y}_i = 0) = W_{pi}(x_0, y_0, 0, 0) + x_i \left(\frac{\partial W_{pi}}{\partial x_i}\right)_0 + \dot{x}_i \left(\frac{\partial W_{pi}}{\partial \dot{x}_i}\right)_0 + \dots \tag{II.9}$$

Restricting ourselves to the first order, we can write the relation (II.9) as follows:

$$W_{pi}(x_0 + x_i, y_0, \dot{x}_i, \dot{y}_i = 0) - W_{pi}(x_0, y_0, 0, 0) = -K_{pi}x_i - C_{pi}\dot{x}_i \tag{II.10}$$

The coefficients K_{pi} and C_{pi} represent the stiffness and damping coefficients due to the existence of the lubricating film in the single-acting hydrostatic thrust bearing $n°$i, in the vicinity of the static equilibrium point.

They are obtained after identification of equations (II.9) and (II.10) as follows :

$$K_{pi} = -\left(\frac{\partial W_{pi}}{\partial x_i}\right)_0 \tag{II.11}$$

$$C_{pi} = -\left(\frac{\partial W_{pi}}{\partial \dot{x}_i}\right)_0 \tag{II.12}$$

The stiffness and damping coefficients are calculated using the numerical differentiation method where the partial derivatives are calculated numerically.

The application of this method involves the following steps:

- Search for the static equilibrium position characterized by (x_0, y_0) .
- Calculate the derivative $\left(\frac{\partial W_{p1}}{\partial x_1}\right)_0$ the equation is solved for the position of the center of the moving grain defined by: $(x_1 = \Delta x_0, y_1 = 0, \dot{x_1} = 0, \dot{y}_1 = 0)$

The integration of the pressure field allows to calculate W_{p1} at this position, thus:

$$K_{p1} = -\frac{\partial W_{p1}}{\partial x_1} = -\frac{W_{p1}\left(x_0 + \Delta x_0, y_0, 0, 0\right) - W_{p1}\left(x_0, y_0, 0, 0\right)}{\Delta x_0} \tag{II.13}$$

- Calculate the derivative $\left(\frac{\partial W_{p1}}{\partial \dot{x}_1}\right)_0$, the equation is solved for each position defined by: $(x_1 = 0, y_1 = 0, \dot{x_1} \neq 0, \dot{y}_1 = 0)$, thus:

$$C_{p1} = -\frac{\partial W_{p1}}{\partial \dot{x}_1} = -\frac{W_{p1}\left(x_0, y_0, \dot{x}_1, 0\right) - W_{p1}\left(x_0, y_0, 0, 0\right)}{\dot{x}_1} \tag{II.14}$$

II.3.2 Equivalent Dynamic Coefficients

The equivalent dynamic characteristics of the bearing are written as follows:

$$K_{eqx} = K_{p2} + K_{p4} \quad ; \quad K_{eqy} = K_{p1} + K_{p3} \tag{II.15}$$

$$C_{eqx} = C_{p2} + C_{p4} \quad ; \quad C_{eqy} = C_{p1} + C_{p3} \tag{II.16}$$

Where K_{eqx} and K_{eqy} represent the equivalent stiffness coefficients in the x and y directions, respectively. While C_{eqx} and C_{eqy} represent the equivalent damping coefficients in the x and y directions, respectively.

The damping ratio ς in the x and y directions is expressed as follows:

$$\varsigma_x = \frac{C_{eqx}}{2\sqrt{MK_{eqx}}} \quad ; \quad \varsigma_y = \frac{C_{eqy}}{2\sqrt{MK_{eqy}}} \tag{II.17}$$

II.4 Flow through thin film

Variable permeability air bearings are a type of air bearing that utilizes a thin film of compressed air to support a load. These bearings find application in various fields like machine tools, vibration isolation platforms, and high-precision guidance systems. The key performance factors for variable permeability air bearings include the air film thickness, supply pressure, and, crucially, the controllable permeability of the supporting surface. Our project focuses on analyzing the flow characteristics within this thin air film specifically in the context of variable permeability

air bearings. By strategically manipulating the permeability of the supporting surface, we aim to optimize airflow and enhance the overall performance of the bearing.

II.4.1 Governing Laws of Thin-Film Flow

In the context of variable permeability air bearings, the flow of air through the thin film is governed by the principles of mass conservation and fluid motion.

The Equation of Continuity

Ensures that the amount of air entering the bearing system is precisely equal to the amount exiting, maintaining a steady air supply.

$$\frac{\partial}{\partial x}(\rho u) + \frac{\partial}{\partial y}(\rho v) + \frac{\partial}{\partial z}(\rho w) + \frac{\partial}{\partial t}\rho = 0 \tag{II.18}$$

The Navier-Stokes Equations

on the other hand, delve into the intricate details of air movement within the thin film, considering viscous forces and inertial effects. These equations allow us to predict the velocity, pressure, and temperature distributions of the air, providing valuable insights into the performance of the air bearing.

Equation development: The Navier-Stokes equation is expressed as follows:

$$\rho\left(\frac{\partial v}{\partial t} + v \cdot \nabla \mathrm{v}\right) = -\nabla \mathrm{p} + \mu \nabla^2 v + f \tag{II.19}$$

where:

- μ : is the velocity field of the fluid
- ρ : is the density of the fluid
- **p** : is the pressure of the fluid
- v : is the kinematic viscosity of the fluid
- **f** : is the body force acting on the fluid

The Navier-Stokes equation comprises these main terms:

- **Inertial Term** $\left(\frac{\partial v}{\partial t}\right)$: This term represents the acceleration of the fluid due to its own velocity and variations in velocity across space.
- **Pressure Term** ($-\nabla p$): This term represents the force exerted by the fluid pressure on fluid elements.
- **Viscous Term** $\left(\mu\nabla^2 v\right)$: This term represents the internal frictional force within the fluid due to its viscosity.
- **Body Force Term (f)**: This term represents any external force applied to the fluid, such as gravity or electromagnetic forces.

To accurately model the air flow within the thin film of a variable permeability air bearing, it is crucial to consider the governing laws of mass conservation and fluid motion. These governing equations can be effectively solved using numerical techniques like the Finite Element Method (FEM) and the Finite Volume Method (FVM). These methods allow us to discretize the bearing system and approximate the flow variables, providing valuable insights into the behavior of the air within the bearing.

Reynolds equation

Its used to determine the thin film pressure field after the porous area. This equation is a case particle Navier-Stokes equations. It is obtained by simplifying the pressio gradients the direction of the thickness of the thin film (here the direction is "y"). Its expression is:

$$\frac{\partial}{\partial x}\left(\frac{h^3}{\mu}\frac{\partial P}{\partial x}\right)+\frac{\partial}{\partial z}\left(\frac{h^3}{\mu}\frac{\partial P}{\partial z}\right)=6U\frac{\partial h}{\partial x}+12\frac{\partial h}{\partial t}. \tag{II.20}$$

The force of lift

noted W is the force generated by the pressure in the aerostatic, which offsets the applied load. To calculate the po force we integrate the pressure field on the lift surface, which is given as follows:

$$W = \iint_{x,y} P(x,y)ds \tag{II.21}$$

If the pressure field is constant or the lift area is small the charge W can be calculated by:

$$W = P_m \times s \tag{II.22}$$

II.5 Simulation of fluid flow through porous media

Numerical methods are a cornerstone for tackling intricate fluid flow challenges within hydrostatic bearings. These methods rely on a process known as discretization, where the computational domain is divided into a mesh of small elements (cells). Subsequently, the governing equations of fluid dynamics, such as the Navier-Stokes equations, are applied to each cell within the mesh.

In popular CFD software like CFX, the finite volume method (FVM) is a prevalent approach for discretizing the flux and source terms present in the conservation equations. These terms are then evaluated on the faces of each cell within the mesh. The discretized equations are then solved iteratively using numerical algorithms to obtain pressure, velocity, and temperature distributions throughout the bearing domain.

FVM offers numerous advantages for hydrostatic bearing simulations, including:

- **Assured global conservation**: The method guarantees that crucial physical quantities, like mass and momentum, are conserved throughout the computational domain.
- **Geometric adaptability**: FVM can effectively handle complex bearing geometries, ensuring accurate representation of the fluid flow characteristics within intricate bearing designs.
- **Versatile boundary condition treatment**: The method is adept at incorporating various boundary conditions, allowing for the simulation of diverse operating scenarios for the hydrostatic bearing.

The overall CFD simulation process involves two key stages:

- **Mesh Generation**: This step subdivides the bearing geometry into a network of control volumes, which form the foundation for the computational domain. The mesh quality significantly impacts the accuracy and efficiency of the simulation.
- **Discretization**: Here, the governing equations are transformed from their continuous form to an algebraic form applicable to each control volume within the mesh. The chosen discretization scheme plays a crucial role in capturing the physics of the flow accurately.

By leveraging numerical methods and CFD tools, engineers can gain valuable insights into the performance of hydrostatic bearings. These simulations enable the prediction of pressure distribution, film thickness, and load-carrying capacity, facilitating the design and optimization of hydrostatic bearings for various engineering applications.

II.5.1 Study of a one-dimensional diffusion problem

Consider a scenario where we want to analyze the transport of a variable through a domain via diffusion.

$$div(\Gamma \text{grad}\ \alpha) + S_\alpha = 0 \tag{II.23}$$

The FVM hinges on the application of the divergence theorem, which allows us to convert a volume integral into a surface integral.

$$\int_{Cv} div\,(\Gamma \text{grad}\ \alpha)\,dv + \int_{Cv} S_\alpha dv = \int_A n\,(\Gamma \text{grad}\ \alpha)\,dA + \int_{Cv} S_\alpha dv = 0 \tag{II.24}$$

Here:

A: Represents the surface enclosing a specific control volume.

n: Denotes the unit normal.

By leveraging the divergence theorem on the diffusion term in the transport equation for a variable we arrive at a discretized form suitable for the FVM approach. This discretized equation in 1D can be expressed as follows:

$$\frac{d}{dx}\left(\Gamma\frac{d\alpha}{dx}\right)+S=0 \tag{II.25}$$

Γ: Represents the diffusion coefficient,

(S): Denotes the source term.

Mesh :

When analyzing fluid flow in one spatial dimension, the computational domain, typically represented by a straight line, is discretized into a collection of regular segments. These segments serve as the control volumes for the one-dimensional case. To illustrate this concept, consider a mesh comprising five control volumes, as shown below:

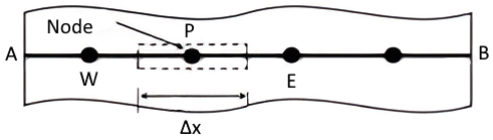

Figure II.2: Schematisation of control volume 1D [1]

Discretization :

The Navier-Stokes equation, which governs the flow of viscous fluids, is discretized using the Finite Volume Method (FVM) within each control volume. The FVM involves integrating the governing equation over each CV and applying appropriate boundary conditions. This process transforms the partial differential equation into a system of algebraic equations that can be solved numerically using computers.

The integration of equation (II.25) on the center control volume P gives:

$$\int \Delta v\frac{d}{dx}\left(\Gamma\frac{d\alpha}{dx}\right)dv+\int_{\Delta v} sdv=\left(\Gamma\frac{d\alpha}{dx}\right)_e-\left(\Gamma A\frac{d\alpha}{dx}\right)_W+\bar{S}\Delta V=0 \tag{II.26}$$

The source term $\bar{S}$ represents the average contribution from external sources within the control volume ”dV.” This term is particularly relevant when analyzing one-dimensional fluid flow scenarios, where the volume is denoted as ”V=X.”

In cases where the diffusion coefficient ”n” is not constant, its values on the ”w” and ”e” faces of the control volume CV depend on the nodal values at points P, W, and E. This non-uniformity in the diffusion coefficient reflects the varying rate at which the quantity diffuses across different regions of the control volume.

$$\Gamma_E = \frac{\Gamma_E - \Gamma_P}{2} \quad \Gamma_W = \frac{\Gamma_P - \Gamma_W}{2}$$

II.5.2 Three-Dimensional Scattering Problem in the Case of a 3D Problem

In the context of three-dimensional (3D) finite volume meshes, each node, denoted by ”P,” has six neighboring nodes. These neighbors are labeled as ”W” (west), ”E” (east), ”S” (south), ”N” (north), ”B” (bottom), and ”T” (top). The corresponding six facets of the control volume associated with node ”P” are designated as ”w,” ”e,” ”s,” ”n,” ”b,” and ”t,” respectively.

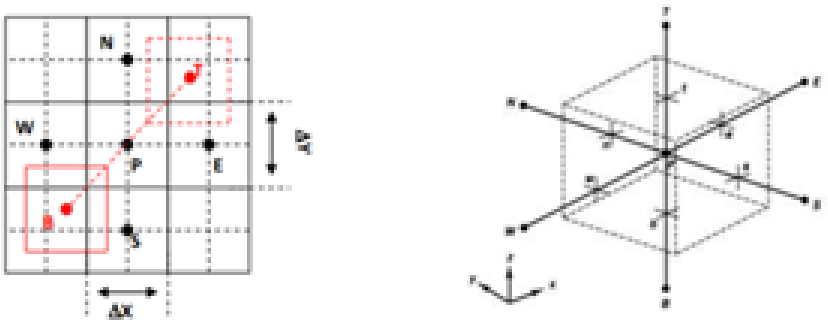

Figure II.3: Schematisation of controle volume 3D [1]

Where:

$$a_W = \frac{\Gamma_W}{\Delta X}\Delta Y \Delta Z \quad a_E = \frac{\Gamma_E}{\Delta X}\Delta Y \Delta Z$$
$$a_N = \frac{\Gamma_N}{\Delta Y}\Delta X \Delta Z \quad a_S = \frac{\Gamma_S}{\Delta Y}\Delta X \Delta Z$$
$$a_B = \frac{\Gamma_B}{\Delta Z}\Delta X \Delta Y \quad a_T = \frac{\Gamma_N}{\Delta Z}\Delta X \Delta Y$$

$$a_P = a_W + a_E + a_N + a_S + a_B + a_T + S_P$$

CHAPTER III

RESULTS AND DISCUSSIONS

Chapter III

RESULTS AND DISCUSSIONS

III.1 Introduction

The main purpose of this chapter is to present the results obtained from our study focusing on the influence or effect of permeability on charge.

III.2 Theoretical model

Our idea in this work is to improve the idea of Xin-Xao in article named “Study on Static Characteristics of Aerostatic Bearing Based on Porous SiC Ceramic Membranes”, in this article Xin-Xao studied the aerostatic pad shown in figure1, both experimentally and theoretically with 3D simulations.

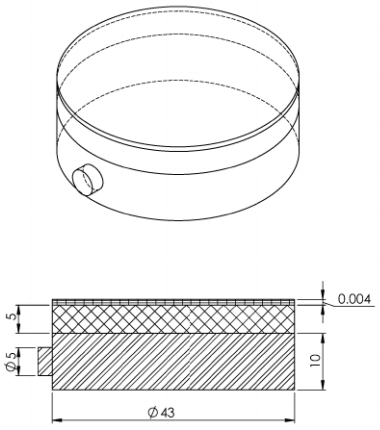

Figure III.1: Theoretical model of Xin Xiao [15]

III.3 Geometry

The structure of an aerostatic bearing is mainly divided into two parts the bearing body and restrictor. For the design of the bearing body according to the design drawing shown in Figure1. The porous restrictor is made of porous SiC (silicon carbide) ceramic.

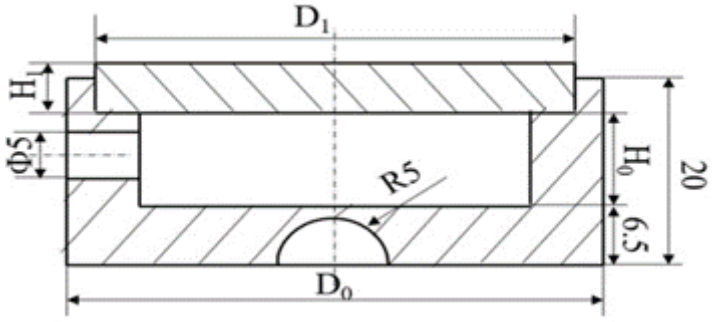

Figure III.2: Xin-Xiao model [15]

So here our reference named “Etude théorique et modélisation des butées poreuses pour le contrôle des vibrations” after using this geometry, they have observed that it can be simplified by eliminating the entire non-porous lower part.

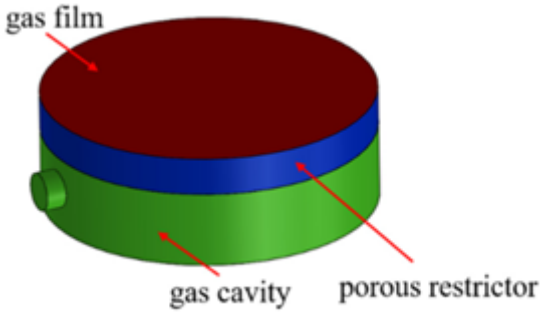

Figure III.3: generic model of Xin-Xao [15]

They studied just the porous zone, and at this point it starts our work by realizing their geometry then cutting the porous zone into two parts. After that we inject by pressing a porous cylinder form into these two parts. As shown in figure:

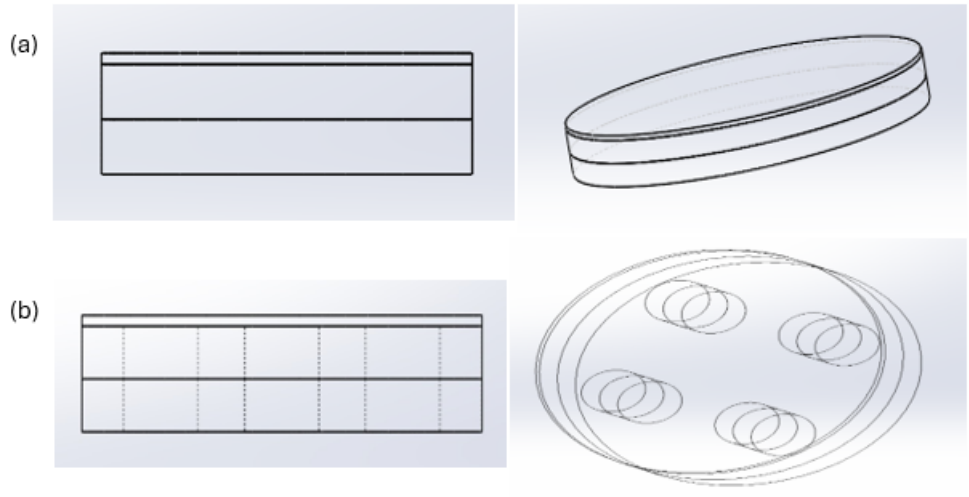

Figure III.4: Our model (a) before, (b) after injecting porous cylinders

III.4 The boundary conditions and hypothesis

Fluid is Newtonian, Viscosity is constant, and the gas is assumed to be ideal, and the flow in the porous zone, inlet, and the gas film is laminar, while the effect of the wall roughness on the gas flow is ignored. The pressure inlet, and pressure outlet are set to 0.5 MPa and 0 MPa, respectively. Two primary characteristics that characterize a permeable substance are its viscous resistance and internal resistance. Specifically, the viscous resistance has been assigned a value of "3.60 × 1012 m-2", however, the internal resistance was not considered.

Parameters	Values
Thickness of gas cavity $(\mathrm{h})(\mu\mathrm{m})$	10
Thickness of porous zone $(\mathrm{H1})(\mathrm{mm})$	5
Diameter of porous zone $(\mathrm{D1})(\mathrm{mm})$	43
Thickness of 2 porous zone after cutting	2.5
Dimeter of cylinders injected $(\mathrm{D2})(\mathrm{mm})$	8
pressure inlet $(\mathrm{Pi})(\mathrm{MPa})$	0.5
Environmental temperature $(\mathrm{T})(\mathrm{K})$	298
Environmental pressure $(\mathrm{P0})(\mathrm{MPa})$	0.1
Aerodynamic viscosity $(\mu)(\mathrm{N}\cdot\mathrm{s}/\mathrm{m2})$	1.7894×10^{-5}
Permeability coefficient of porous medium $(\phi)(\mathrm{m2})$	2.78×10^{-13}

Table III.1: boundary conditions [16]

III.5 Model and meshing

The mesh is adopted of type structured, and due to the curvature of the geometry, we divided it to prevent highly deformed elements.

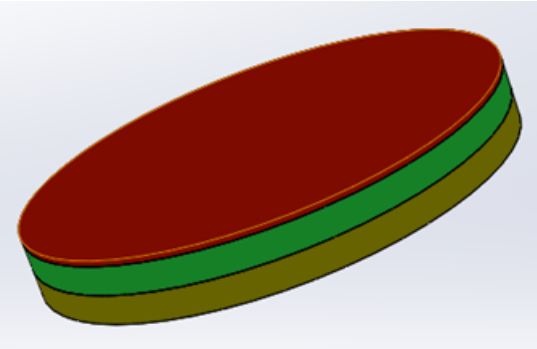

Figure III.5: Model before injecting cylinders

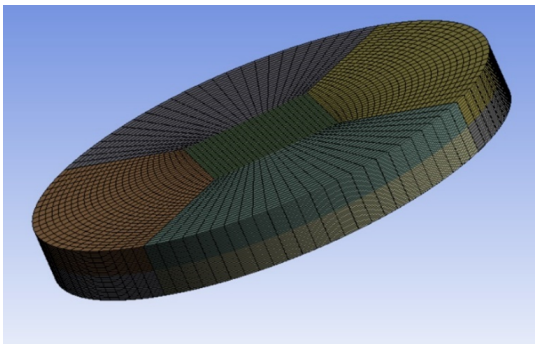

Figure III.6: Meshing of model

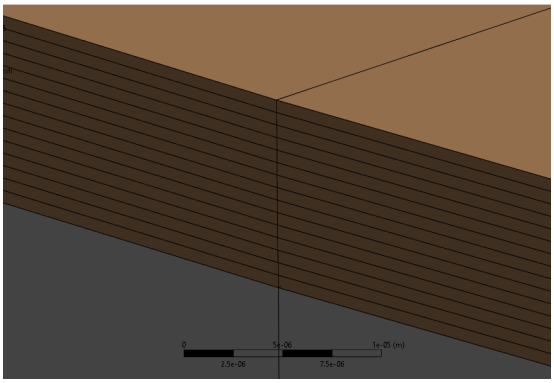

Figure III.7: Meshing of air film

III.6 Statistics of meshing for geometry

From the table below and according to “skewness” in “ANSYS MESHING”, we can say that our meshing is better than both of references.

	Our model	Xin-Xao model	Model ”reference”
Nodes	724288	77618	44902
Elements	171875	90475	40000
Average ”skewness”	$7.74e^{-2}$	0.14451	$8.61e^{-2}$
Max ”skewness”	0.5	0.82478	0.5

Table III.2: represents statistic of meshing for different geometries [16]

III.7 Validation

The Darcy law for h = 10 µm and experimental results by:Xin-Xao [15], are used to validate the model we adopted for our study. The pressure difference on either side of the aerostatic pad is used to study the variation of volume flow at the outlet. The figure below provide a description of the results.

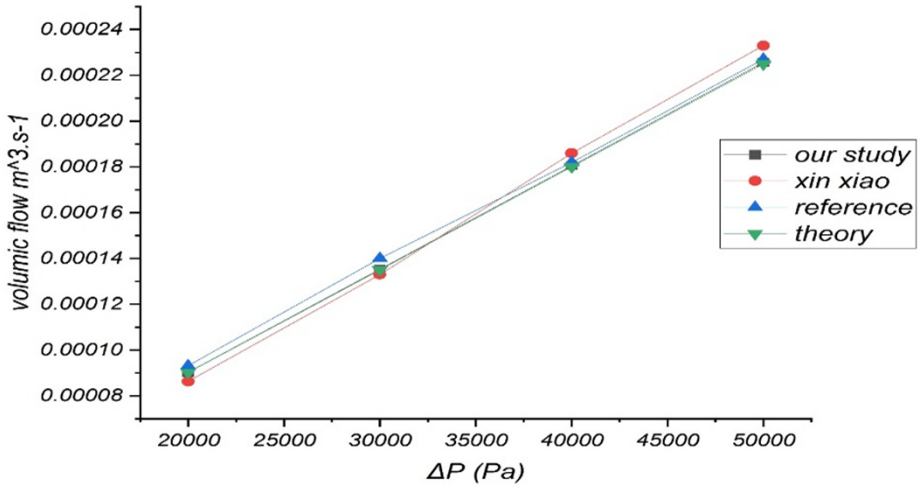

Figure III.8: Graph represents mass flow based on differential in pressure

We can say that the following results its very close to being the same as theoretical result, and when compared to Xin Xiao’s experimental findings, will further support the validity of the adopted model.

III.7.1 Standard deviation

	Volumetric flow rate			Error	
ΔP(Pa)	Theory	Xin xiao	Our study	our study %	Xin Xiao %
20000	$9.02E-05$	8.63E-05	$9.03E-05$	0.06	4.32
30000	$1.35E-04$	$1.33E-04$	$1.35E-04$	0.22	1.48
40000	$1.80E-04$	$1.86E-04$	$1.81E-04$	0.28	3.33
50000	$2.25E-04$	$2.33E-04$	$2.26E-04$	0.27	3.56
Median				0.24	3.44
Standard deviation				0.09	1.04

Table III.3: Table of error comparison

The table compares the theoretical volumetric flow rate with the simulation results obtained in our study and Xin Xiao. It's clear that our simulation results are generally closer to the theoretical values than Xin Xiao's results, with a median percent error of 0.24% compared to 3.44% for Xin Xiao.

III.8 Simulation analysis

III.8.1 Contour of pressure

The pressure contour plot visualizes the distribution of air pressure within the porous bearing. The color gradient, typically ranging from blue (low pressure) to red (high pressure), allows to identify regions with varying pressure levels.

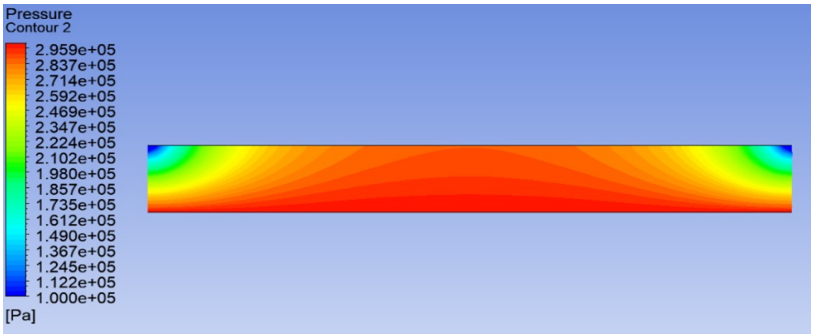

Figure III.9: Simplified model

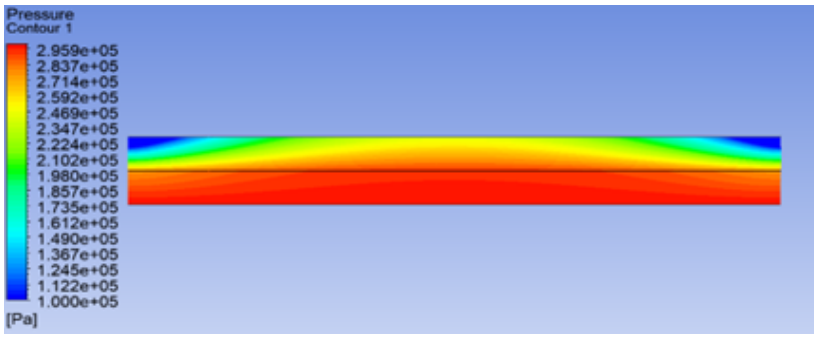

Figure III.10: Model with two porous zones

By comparing between this two contours we can say that the presence of two distinct permeability zones within the porous material will significantly impact this pressure distribution.

At the interface between the two permeability zones, the pressure contours will likely exhibit a discontinuity. This discontinuity arises because the rate of air flow through the porous material is directly related to its permeability. A zone with higher permeability allows for easier air passage, leading to a steeper pressure gradient compared to the lower permeability zone.

The specific shape and location of the permeability zones within the bearing will also influence the pressure distribution and its impact on load capacity. Analyzing the pressure contours in conjunction with the bearing geometry can provide valuable insights.

III.8.2 Effect of permeability into charge

After results shown in the table below and contours of pressure before, we remarque that when we change the permeability of one of porous zone, the charge changes so we got an idea, which is to have 4 porous cylindrical bodies with different permeabilities, in each of our layers so when having different orientations we get a different flow resistance.

Inlet pressure	$3e^5$	$3e^5$	$3e^5$	$3e^5$
Permeability 1	$2.78e^{-13}$	$2.78e^{-13}$	$2.78e^{-14}$	$2.78e^{-14}$
Permeability 2	$2.78e^{-13}$	$2.78e^{-14}$	$2.78e^{-13}$	$2.78e^{-14}$
CHARGE	335.87	238.54	174.77	179.5

Table III.4: represents effect of permeability into charge [16]

III.9 Model with porous cylindrical bodies

Pictures below shown our model after adding the 4 cylindrical forms in each porous layer (to information we studied in 2 cases: aligned, not-aligned).

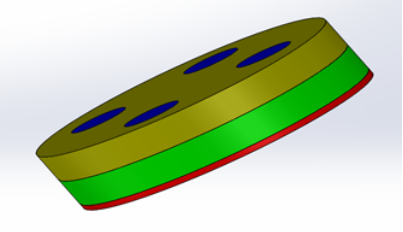

Figure III.11: Final model

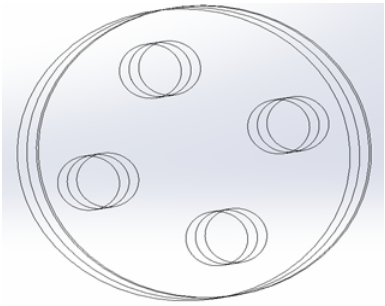

Figure III.12: Model with porous cylindrical bodies aligned

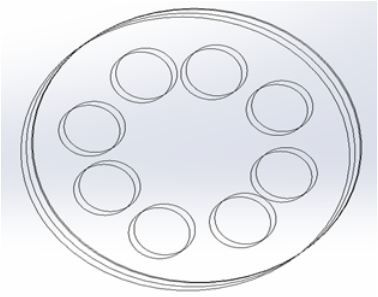

Figure III.13: Model with porous cylindrical bodies not-aligned

III.10 Investigating the impact of cylindrical form alignment in porous aerostatic bearings

The alignment of the cylindrical forms, can influence the pressure and velocity distribution and consequently, the load capacity.

III.10.1 Influence of Cylindrical forms Alignment on pressure

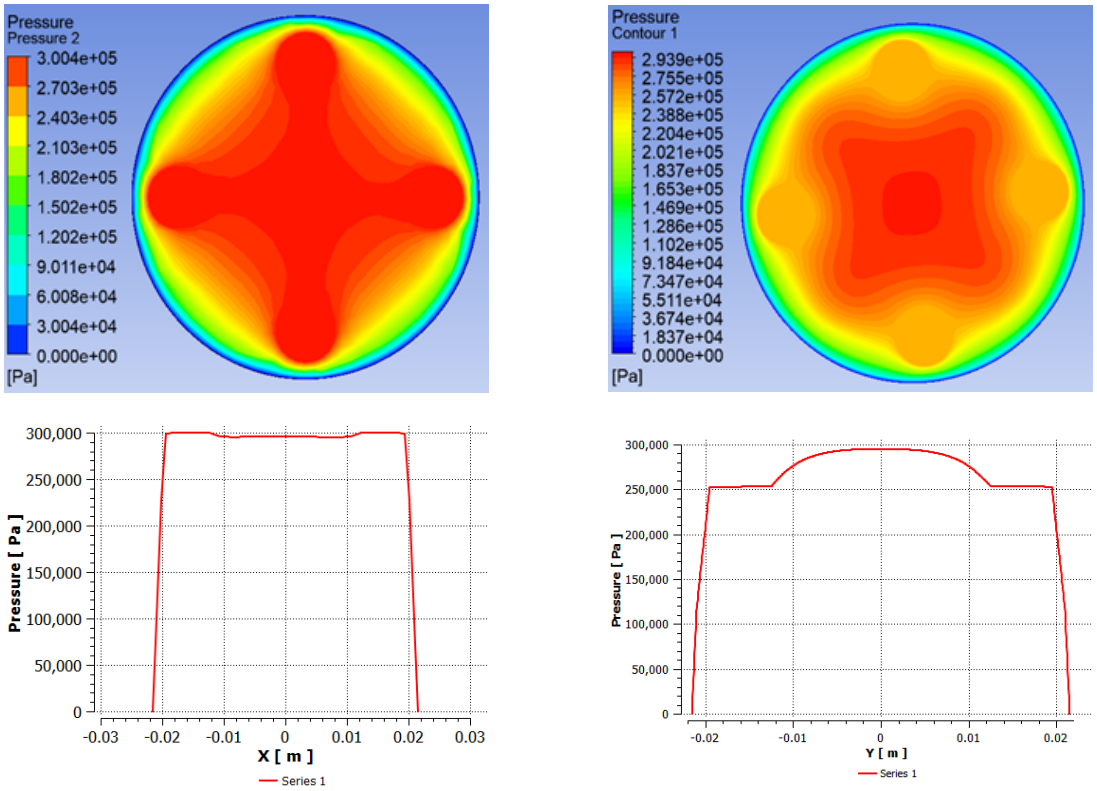

(a) (b)

Figure III.14: Porous cylindrical forms (aligned, not aligned).

So here we will study it in two cases :

1. **Aligned (a)**: When the cylindrical forms are aligned, the pressure contours might show a more channeled flow pattern due to the combined effect of the high permeability of cylindrical forms. This could potentially create a more uniform pressure distribution along the shaft axis, influencing the load capacity in that direction.

2. **Non-Aligned (b)**: With non-aligned cylindrical forms, the pressure contours might exhibit a less organized pattern due to the varying flow paths created by the arrangement of the cylindrical forms. This could lead to a more non-uniform pressure distribution along the shaft axis, potentially affecting load capacity in that direction.

III.10.2 Influence of Cylindrical forms Alignment on Velocity

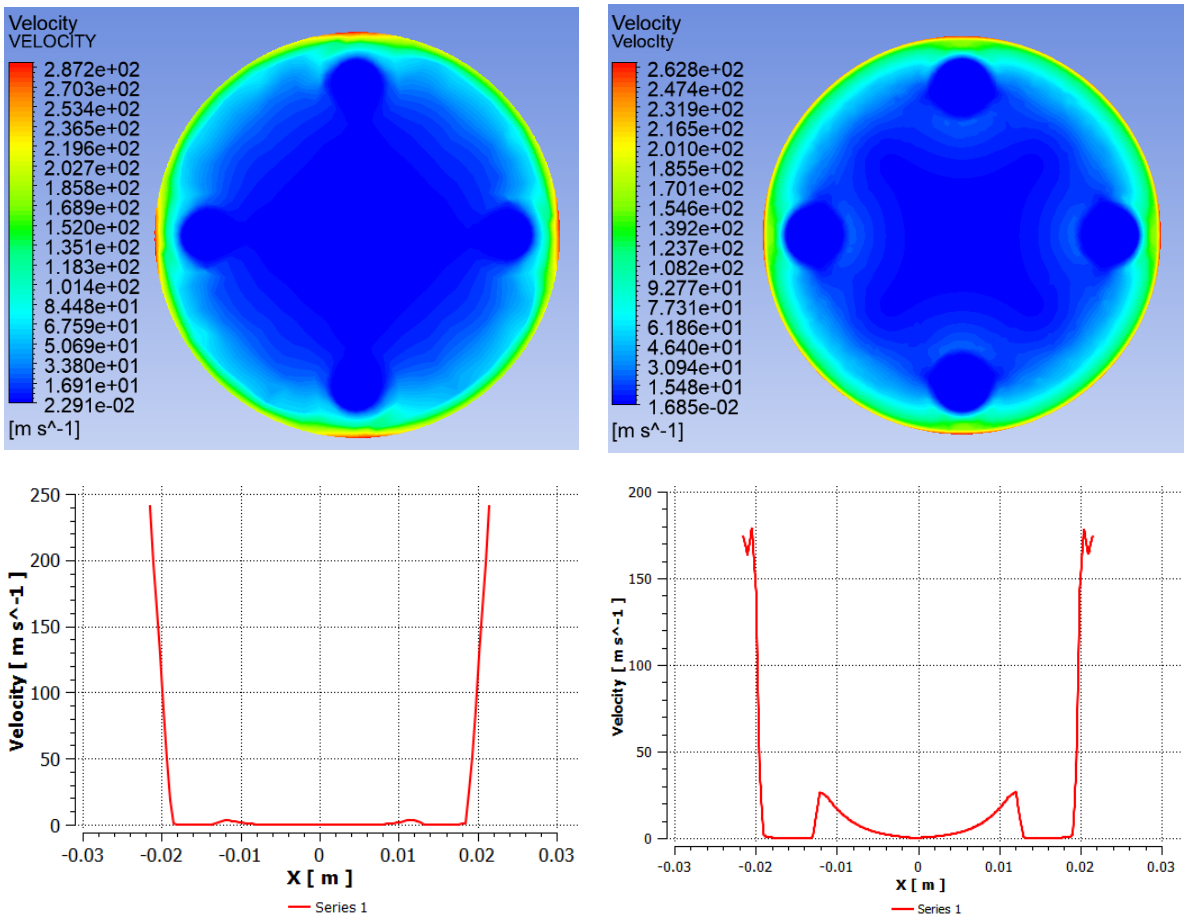

(a) (b)

Figure III.15: Porous cylindrical forms (aligned, not aligned).

Like pressure we will study it in two cases :

1. **Aligned (a)**: Due to the high permeability of the cylindrical forms, the regions surrounding them exhibit the highest velocities (denser color gradients). Additionally, the aligned arrangement promotes a more streamlined flow. This translates to denser velocity contours concentrated along the cylindrical forms, suggesting a well-organized flow path.

2. **Non-Aligned (b)**: With non-aligned cylindrical forms, the high-velocity zones (denser contours) become more scattered. The flow encounters varying resistances depending on the cylindrical forms location and orientation, leading to a more complex flow pattern. This complexity is reflected in the velocity contours, which display a less organized distribution with intermixed areas of high and low velocity throughout the bearing.

III.11 Effect of different permeabilities on charge in the final model

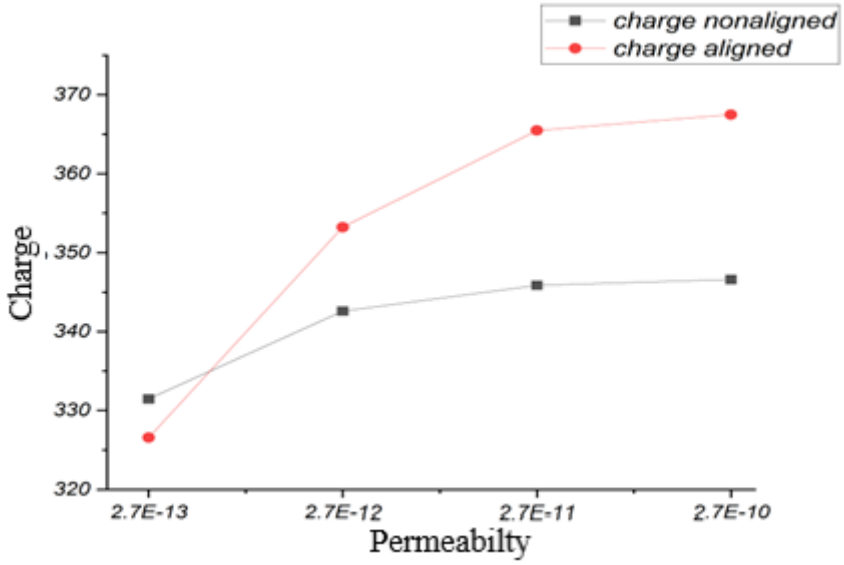

Figure III.16: Effect of different permeabilities into charge

We can see that what we expected and what we talk about it in Figure III.14 has happened and the aligned cylinders model produced a bigger force compared to the non-aligned one with a difference in force exceeding 20 N.

III.12 Influence of permeability on the dynamic behavior of the bearing:

To study the influence of permeability on the dynamic behavior of the bearing supporting a load, We will consider two cases:

1. **Aligned cylinders :** where the high permeability cylinders are aligned with each other.
2. **Nonaligned cylinders :** where the high permeability cylinders are not aligned with each other with an angle of difference of 45 degrees.

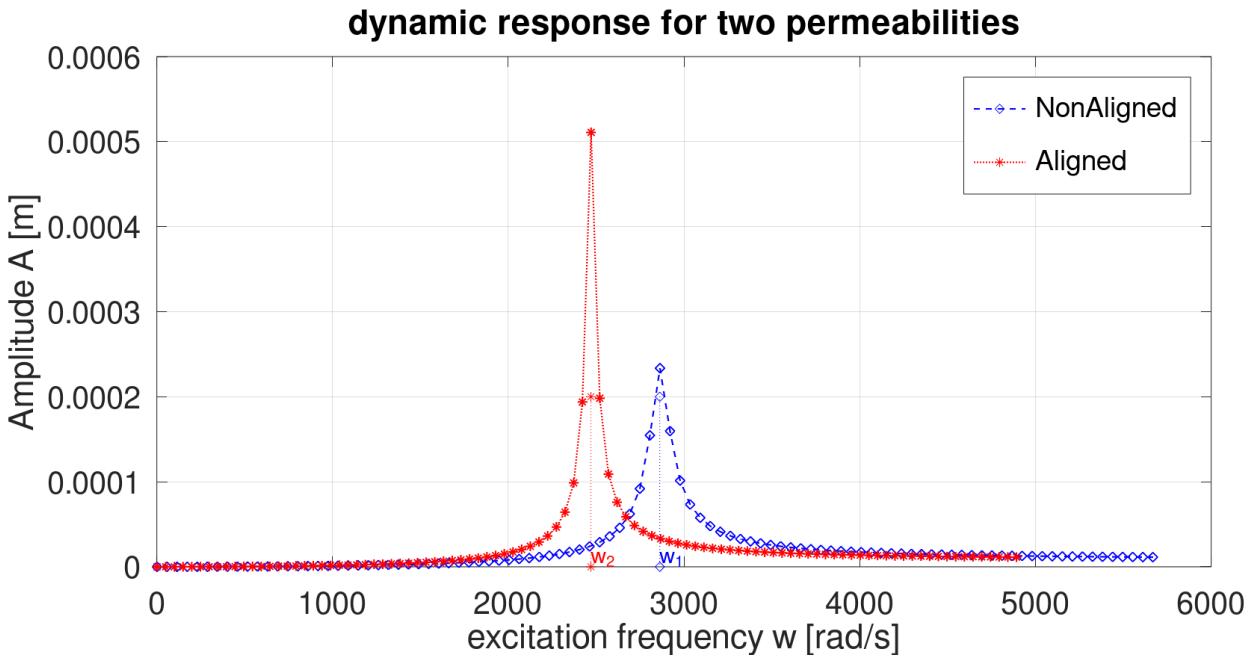

Figure III.17: Vibration amplitude as a function of excitation frequency

When we move to a nonaligned position the stiffness increases and that shifts the natural frequency to the right and that's a very interesting behavior from the bearing because we can dynamically change the cylindrical forms rotation while the system is running and with that so we can change the natural frequency of the system and significantly reduce the vibrations thus avoiding damage to our equipment.

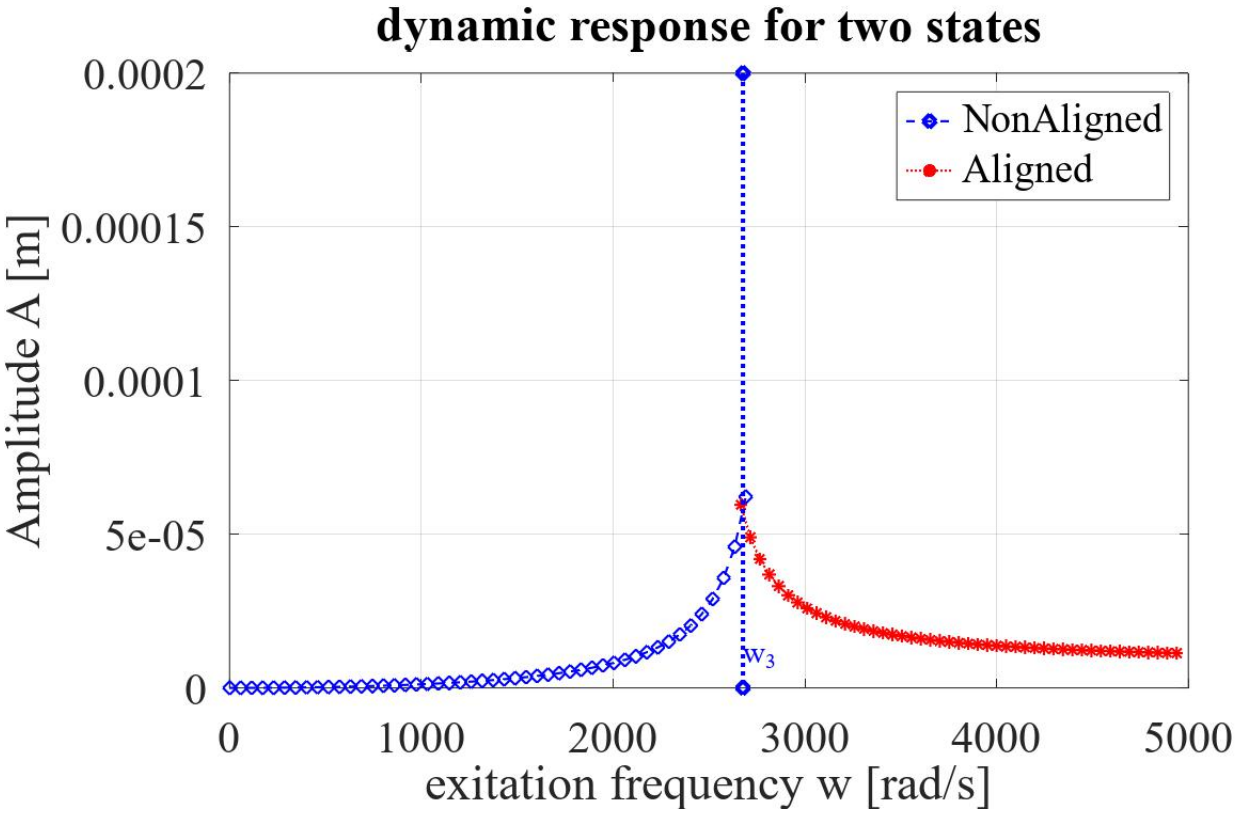

Figure III.18: Vibration amplitude as a function of excitation frequency when we move cylindrical forms with 45 degrees.

We can see that dynamically changing the bearing state can reduce the vibration amplitude.

CONCLUSIONS AND PROSPECTS

CONCLUSIONS AND PROSPECTS

This work aimed to understand how manipulating permeability and design aspects of porous aerostatic bearings can optimize the dynamic stability of rotors they support.The study employed Ansys-CFX, a commercial 3D computational fluid dynamics (CFD) software, for the simulations.

Our initial findings confirmed the chosen model's accuracy. Predicted mass flow closely matched established theoretical models and existing experimental data, suggesting the model's effectiveness for analyzing porous aerostatic bearings.

Our analysis revealed that distinct permeability zones within the porous material significantly impact the pressure distribution across the bearing surface. This variation in permeability manifests as discontinuities in the pressure contours, highlighting the presence of differing flow rates through these zones.

This study unveils a remarkable finding: the dynamic manipulation of permeability, achieved by altering the positioning of cylindrical inserts, offers a novel approach to controlling rotor vibrations. By strategically modifying the permeability distribution, we can steer the rotor's dynamic behavior away from its natural frequencies, effectively mitigating resonant vibrations.

Appendix A

Annexe A

BMC

BUSINESS MODEL CANVAS

TechnoFoster

نموذج مخطط الأعمال للمشاريع الخاصة بالقرار 1275

Presentation 2024

المحتوى

ما هو مشروعك؟

يتناول هذا المشروع اختراعًا مبتكرًا للتحكم في اهتزازات القطع الميكانيكية عن طريق ضبط نفاذية المحامل المسامية . يعتمد هذا النظام على محمل هوائي (أو هيدروستاتيكي) مزود بطبقتين مساميتين متميزتين (يمكن تطبيق المبدأ على طبقات متعددة لمزيد من التحكم) ، تحتوي كل طبقة على العديد من الأشكال المضمنة (عن طريق التثبيت) والتي يمكن أن تكون ذات هندسة متنوعة (أسطوانية في المثال المقترح) .تتمتع الطبقات والأشكال التي تحتوي عليها بنفاذية مختلفة .

يكمن الابتكار في القدرة على ضبط النفاذية الكلية للمحمل عن طريق تعديل زاوية دوران إحدى الطبقات (باستخدام محرك خطوي أو سيرفومحرك) ، وبالتالي محاذاة الأشكال المضمنة في هذه الطبقة مع تلك الموجودة في الطبقة الثانية.

لماذا مشروعك؟

تعتمد أجهزة التحكم في اهتزازات القطع الميكانيكية بشكل عام على تقنيات ميكانيكية معقدة أو أنظمة تعويض يمكن أن تكون باهظة الثمن أو صعبة التنفيذ. ومع ذلك ، فإن حلنا يتضمن فقط العناصر التالية :

- **محمل هوائي :**هذا عنصر دعم يستخدم طبقة هوائية لتقليل الاحتكاك بين سطحين متلامسين. يتكون المحمل الهوائي من غرفة يتم حقن الهواء المضغوط فيها.
- **طبقتان مساميتان :**تنقسم غرفة المحمل الهوائي إلى منطقتين نفاذيتين. تتكون كل منطقة من طبقة مسامية ذات أشكال أسطوانية ذات نفاذية مختلفة.
- **نظام التحكم في النفاذية :**يتم إنشاء نظام لضبط نفاذية إحدى الطبقات المسامية. يمكن أن يكون هذا النظام عبارة عن محرك خطوي يسمح بتغيير زاوية دوران الطبقة المسامية عن طريق التزاوج (الترس ، الحزام ...).

يعتمد مبدأ تشغيل الجهاز على تغيير نفاذية الطبقات المسامية. من خلال تعديل نفاذية المحمل الهوائي ، يتم التأثير على تدفق الهواء عبره وبالتالي تغيير معاييره الديناميكية (الصلابة والتخميد المكافئ).

القيمة المضافة

- يُظهر الجهاز فعالية استثنائية في امتصاص الاهتزازات، مما يؤدي إلى تحسين كبير في أداء الماكينات.
- يعتمد الجهاز على مبدأ جديد لضبط النفاذية باستخدام دوران طبقات مسامية، مما يسمح بتحكم دقيق في امتصاص الاهتزازات .
- يمثل هذا الابتكار نقلة نوعية في مجال التحكم بالاهتزازات، حيث يوفر فاعلية وكفاءة غير مسبوقة.
- على الرغم من كونه تقنية مبتكرة، إلا أن الجهاز يتميز بتكلفة تصنيع معقولة نسبيًا مقارنةً ببدائل التحكم في الاهتزازات الأخرى.
- **القيمة الأمنية :**يُعزز الجهاز السلامة في مكان العمل من خلال تقليل مخاطر الاهتزازات على العمال والمعدات.

شرائح العملاء أو الزبائن Customer Segments

- **المصنعون الصناعيون:** الشركات التي تصنع الآلات بأجزاء دوارة أو مهتزة، مثل مولدات الطاقة والمضخات
- **شركات تصنيع الأجهزة الطبية** وشركات التي تعتمد على **الدقة العالية**.
- **شركات النفط والغاز**: الشركات التي تشغل آبار وخطوط أنابيب النفط والغاز
- **شركات الطيران والدفاع:** الشركات التي تصمم وتصنع الطائرات، والتي تتعرض للاهتزاز من المحركات والأجزاء المتحركة الأخرى

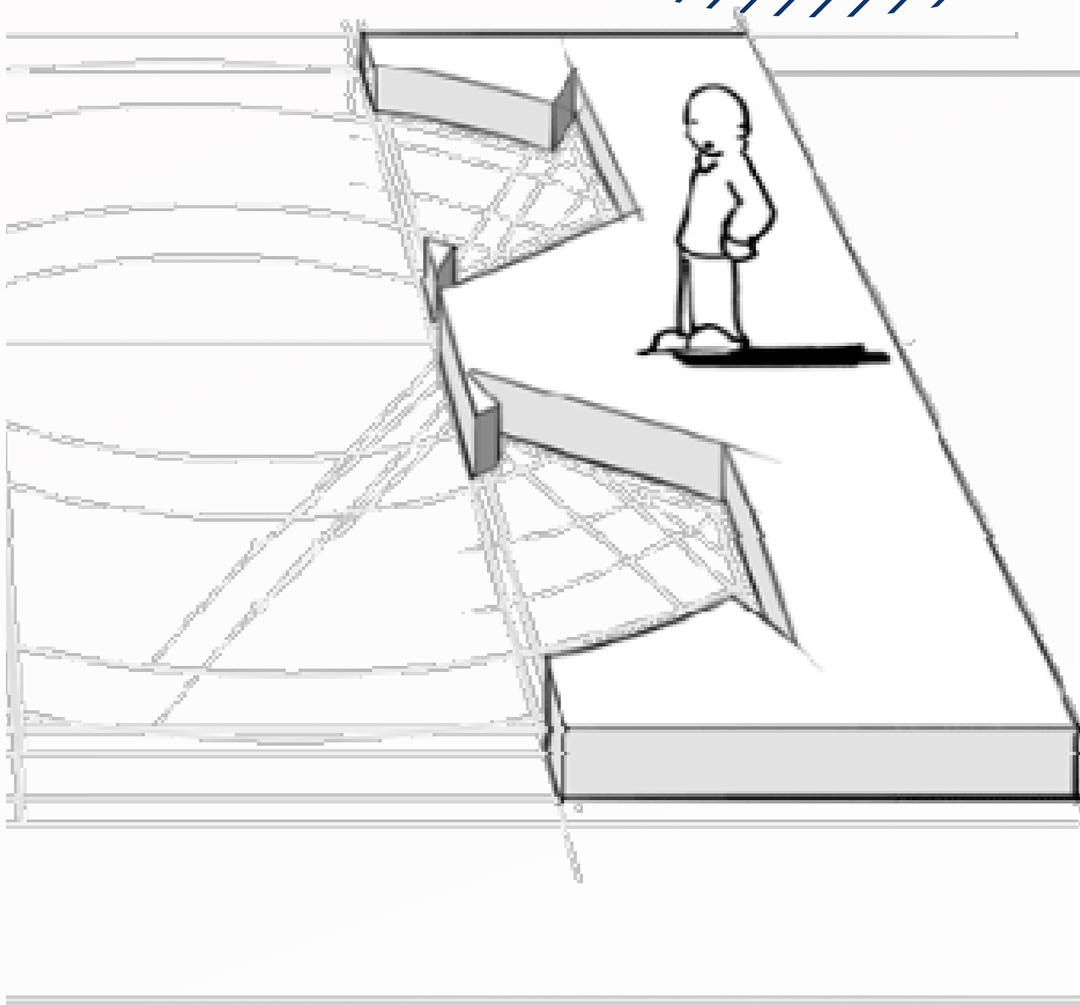

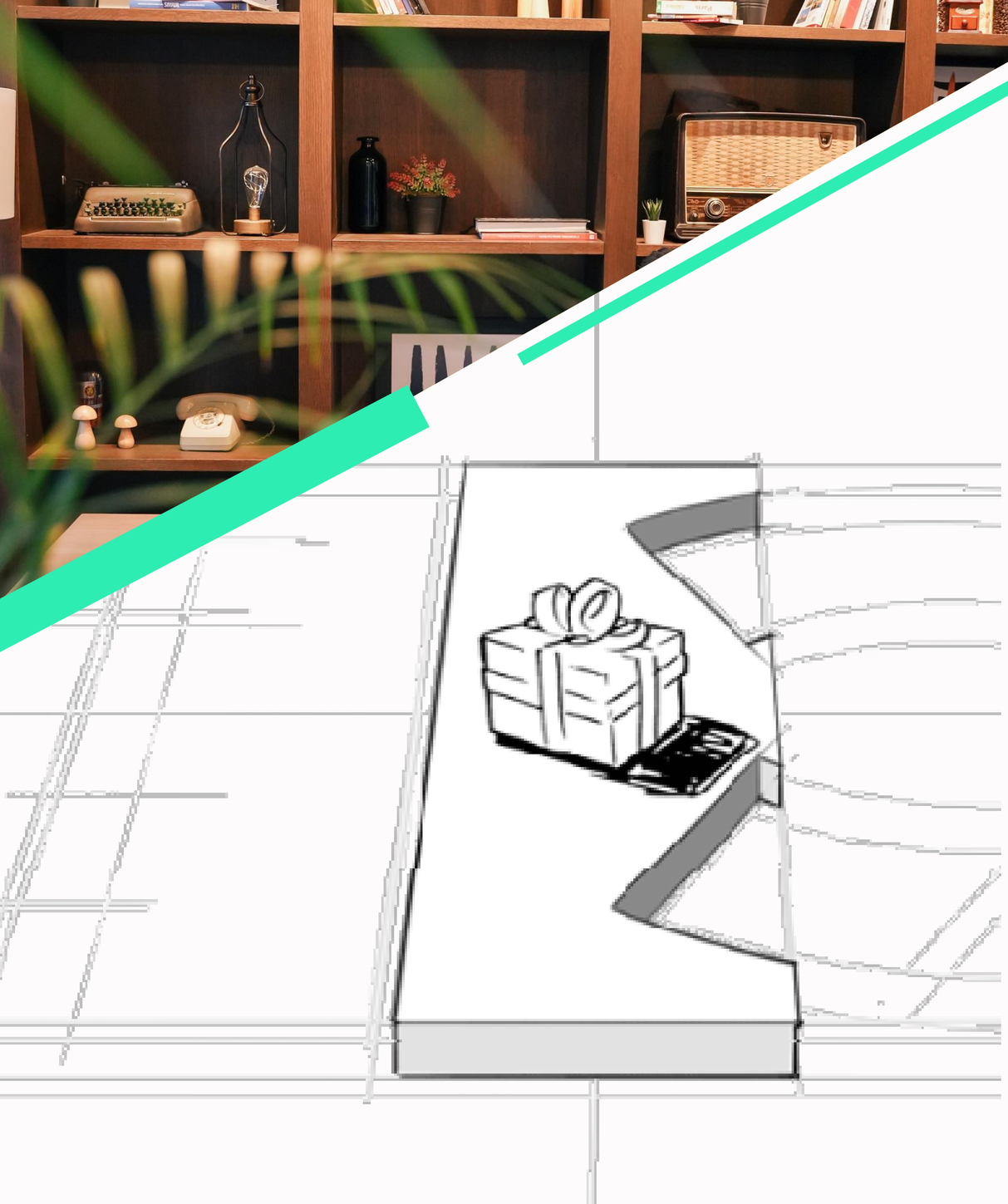

القيمة المقترحة

- **تقليل الاهتزاز:** تقليل الاهتزاز في الآلات، مما قد يؤدي إلى إطالة عمر المعدات، وتقليل مستويات الضوضاء.
- **تحسين كفاءة الطاقة:** من خلال تقليل الاهتزاز، يمكن للجهاز المساعدة في تحسين كفاءة الطاقة في الآلات، مما يؤدي إلى جودة منتج أعلى وتقليل الخسائر.
- **انخفاض تكاليف الصيانة:** من خلال تقليل الاهتزاز على الآلات، يمكن أن يساعد الجهاز في تقليل تكاليف الصيانة.
- **تعدد الاستخدامات:** يمكن تكييف الجهاز مع مجموعة واسعة من الأجزاء والتطبيقات الميكانيكية.

القنوات

1. **المبيعات المباشرة**: تباع مباشرة للمصنعين الصناعيين.
2. شركاء التوزيع
3. المبيعات عبر الإنترنت
4. **الشراكات التقنية:** التعاون مع الشركات الهندسية والاستشاريين لدمج الجهاز في تصميماتهم

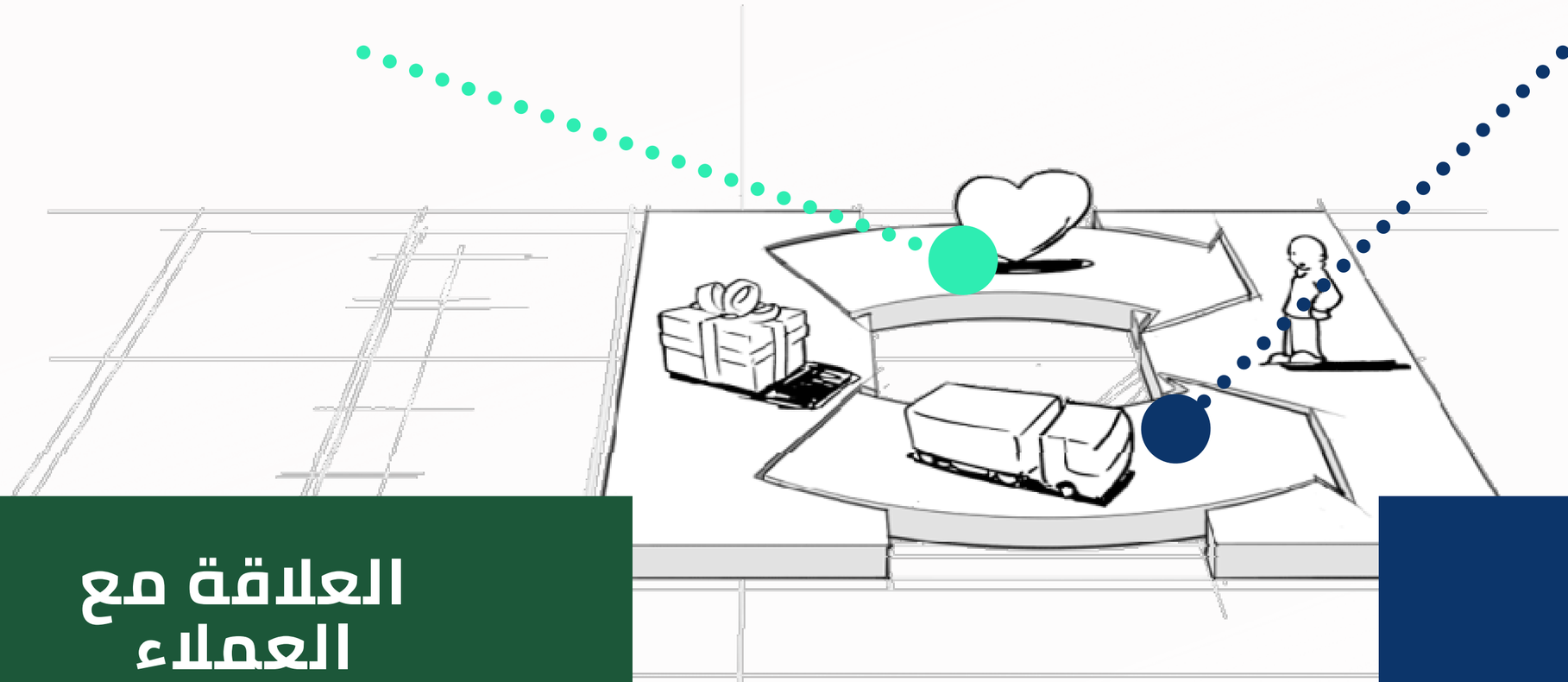

العلاقة مع العملاء

1. خدمة العملاء
2. الدعم التقني
3. التدريب
4. ملاحظات العملاء

مصادر الدخل (الإيرادات)

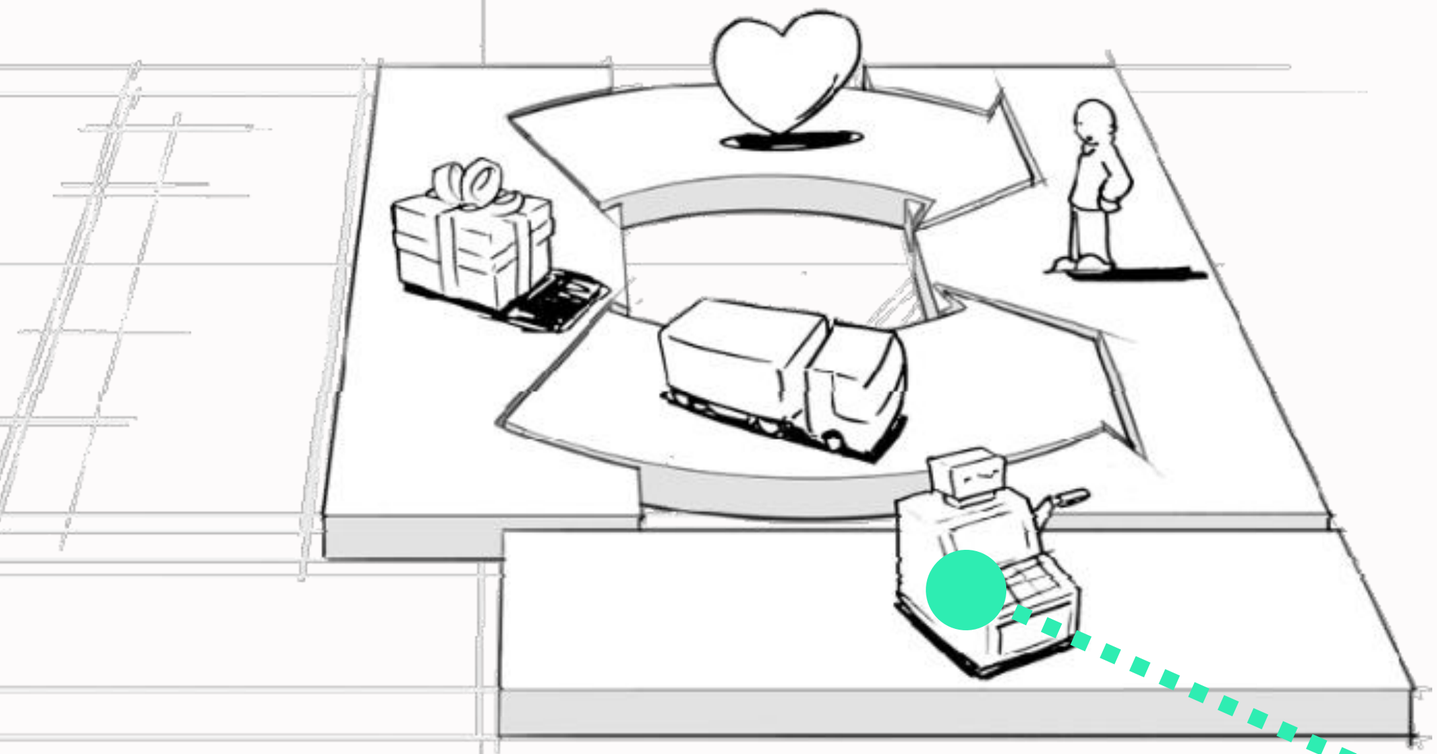

1. **مبيعات الجهاز:** الإيرادات الناتجة عن بيع الجهاز للعملاء.
2. **رسوم الترخيص**: الإيرادات الناتجة عن ترخيص التكنولوجيا لشركات أخرى.
3. **عقود الصيانة**: تقديم عقود صيانة لضمان الأداء الأمثل للجهاز.
4. **التدريب والشهادة:** فرض رسوم على برامج التدريب وإصدار الشهادات لموظفي العملاء.
5. **خدمات تحليل البيانات:** توفير خدمات تحليل البيانات للعملاء لمساعدتهم على تحسين أداء آلاتهم.

المهام (الأنشطةُ) الأساسية

- تطوير المنتج
- دعم العملاء
- التصنيع
- التسويق والمبيعات
- البحث والتطوير

الموارد الرئيسية

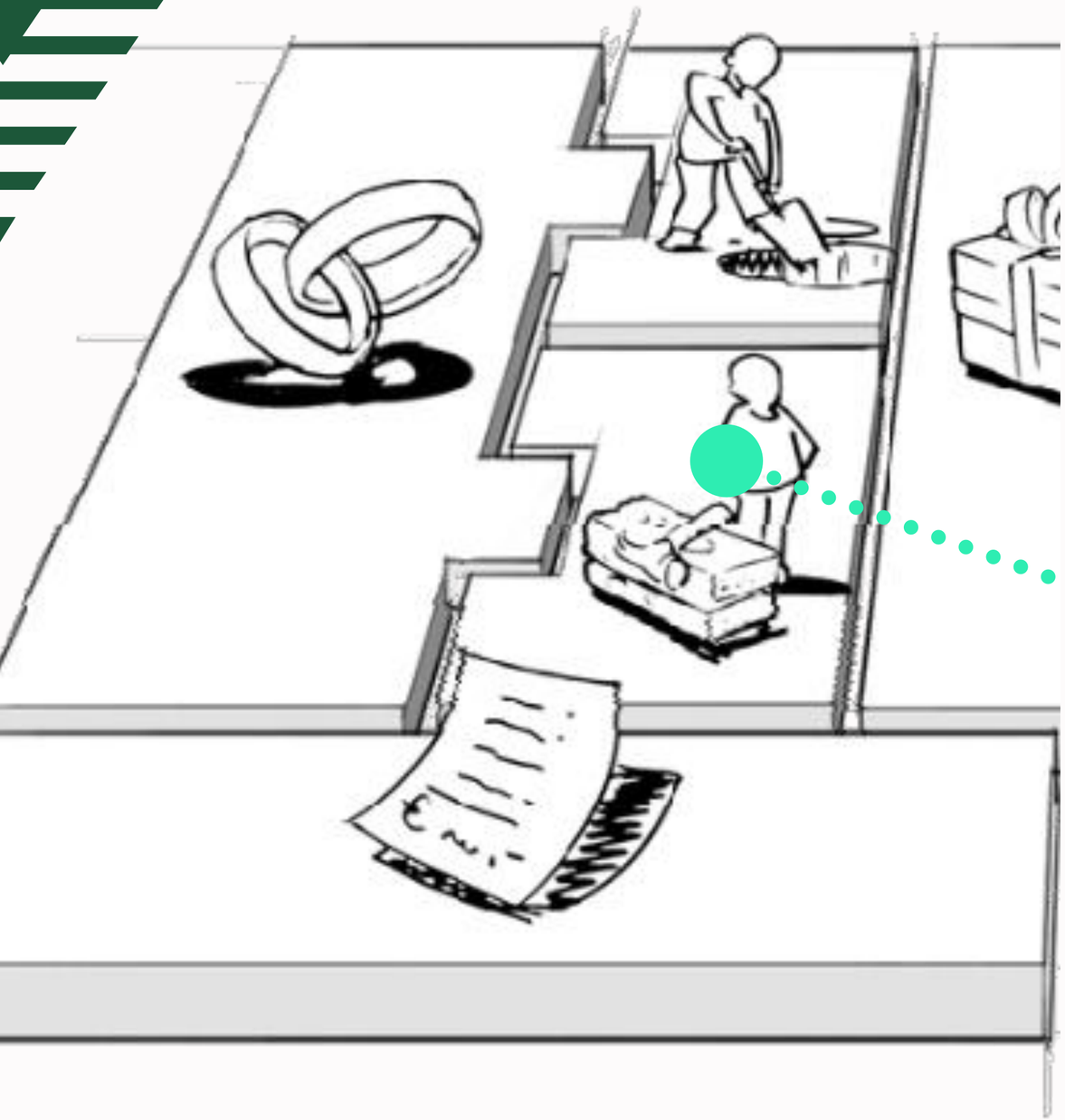

- **مرافق التصنيع** : الات الخراطة و التفريز
- **البحث والتطوير**: الإبقاء على فريق قوي للبحث والتطوير.
- الخبرة التقنية.

الشركاء الرئيسيَّين

- **الموردون**: تتعاون الشركة مع الموردين للحصول على المواد الخام والمكونات اللازمة لتصنيع الجهاز.
- **المؤسسات البحثية:** تتعاون الشركة مع المؤسسات البحثية لتطوير تقنيات جديدة ومحسنة لمكافحة الاهتزازات.
- **شركاء التوزيع:** التعاون مع الموزعين للوصول إلى قاعدة عملاء أوسع.
- **الشركات الهندسية**: الشراكة مع الشركات الهندسية لدمج الجهاز في تصميماتها.

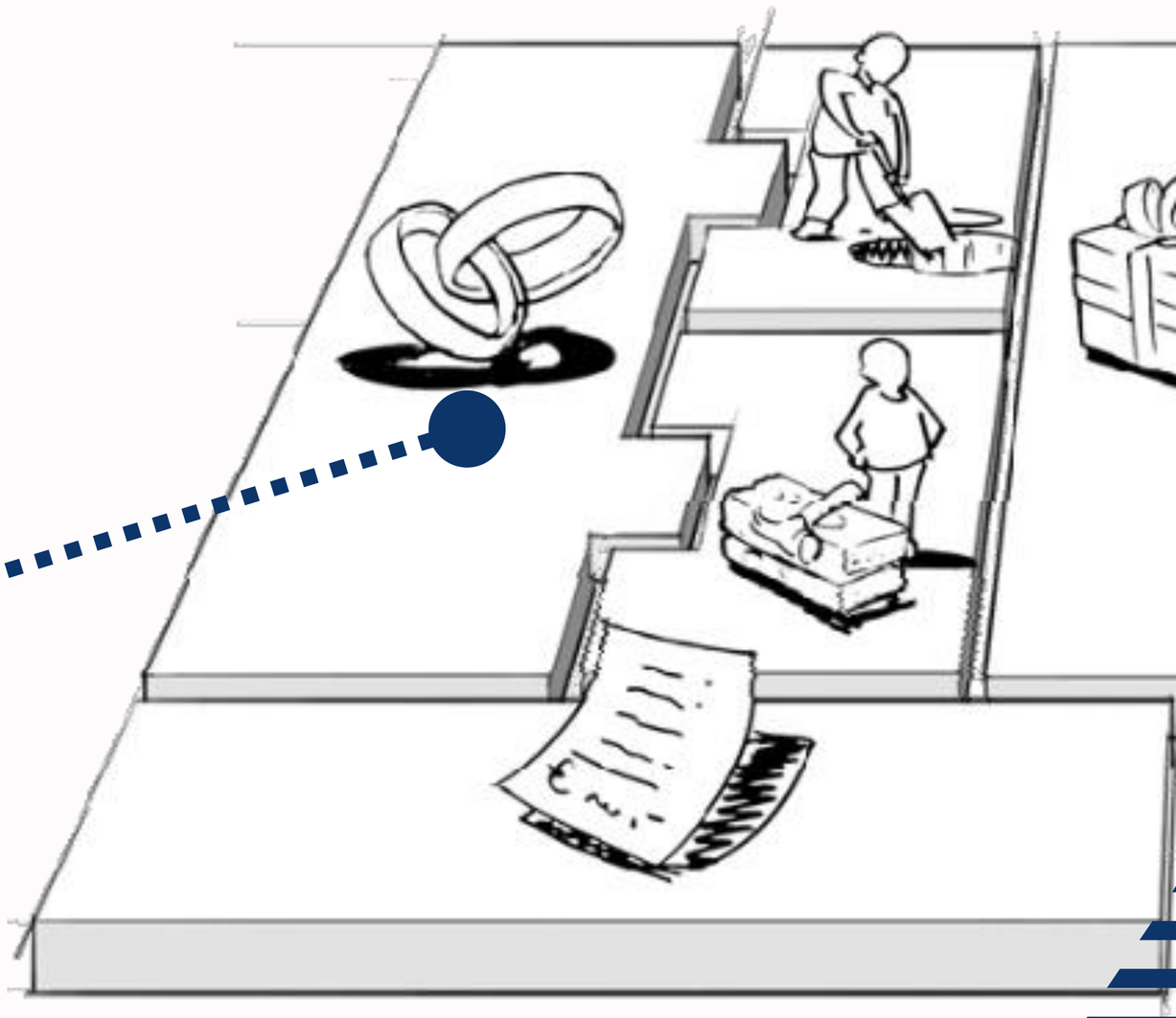

هيكل التكاليف

- **تكاليف التصنيع**: تكاليف المواد الخام والعمالة والنفقات العامة المرتبطة بتصنيع الجهاز.
- **تكاليف التسويق والمبيعات:** تكاليف تسويق وبيع الجهاز.
- **تكاليف دعم العملاء**: تكاليف توفير الدعم التقني وخدمة العملاء.
- **التكاليف العامة والإدارية:** التكاليف العامة مثل المرتبات والإيجار والمرافق العامة.

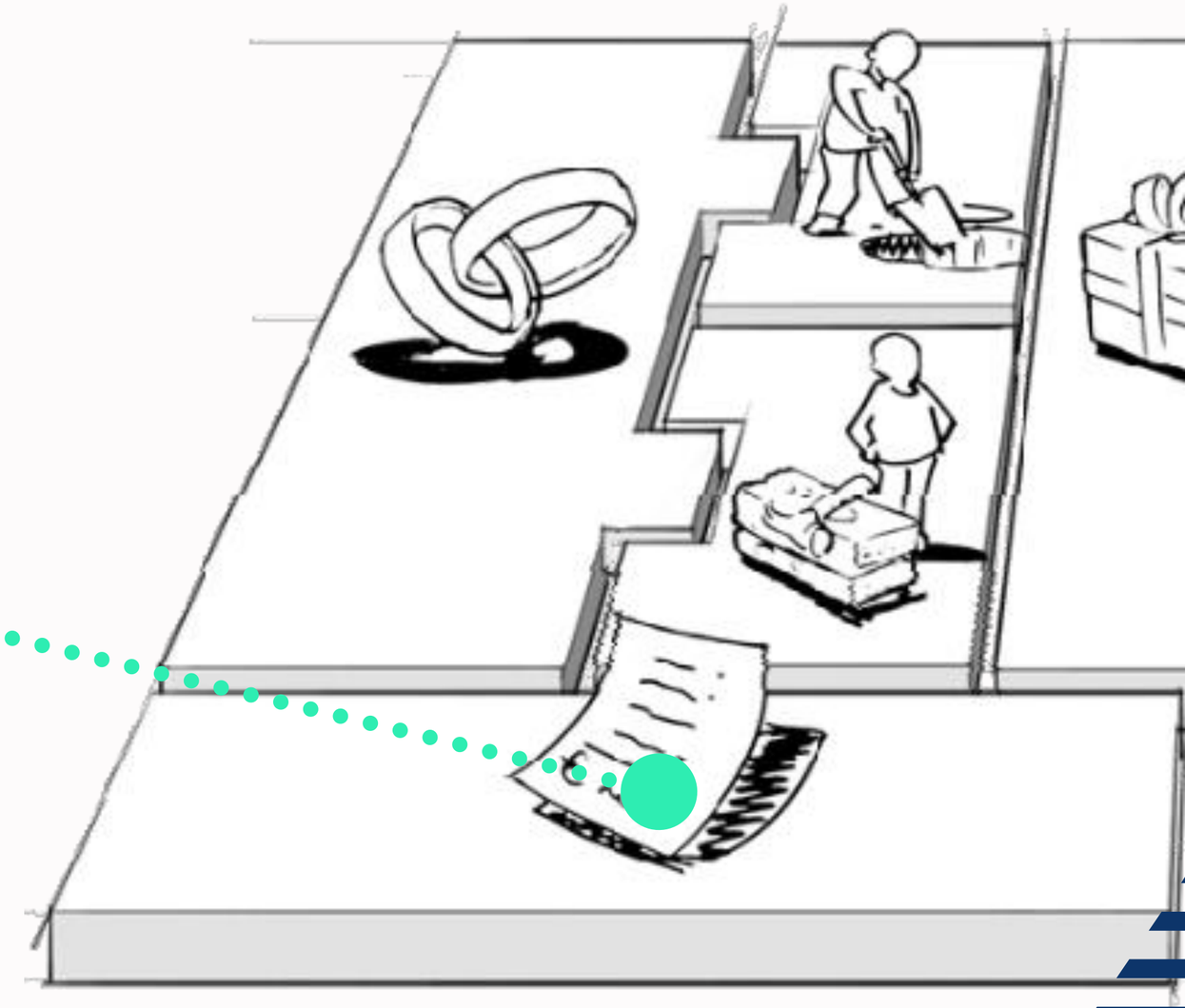

Business Model Canvas

Desianed for:	Desianed bu:	Date:	Version:

الشركاء الرئيسيون	الأنشطة الرئيسية	عروض القيمة	علاقات العملاء	شرائح العملاء
• الموردون: تتعاون الشركة مع الموردين للحصول على المواد الخام والمكونات اللازمة لتصنيع الجهاز. • المؤسسات البحثية: تتعاون الشركة مع المؤسسات البحثية لتطوير تقنيات جديدة ومحسنة لمكافحة الاهتزازات. • شركاء التوزيع: التعاون مع الموزعين للوصول إلى قاعدة عملاء أوسع. • الشركات الهندسية: الشراكة مع الشركات الهندسية لدمج الجهاز في تصميماتها.	• تطوير المنتج • دعم العملاء • التصنيع • التسويق والمبيعات • البحث والتطوير **الموارد الرئيسية** • مرافق التصنيع.الات الخراطة... • البحث والتطوير: الإبقاء على فريق قوي للبحث والتطوير. • الخبرة التقنية.	• تقليل الاهتزاز: تقليل الاهتزاز في الآلات، مما قد يؤدي إلى إطالة عمر المعدات، وتقليل مستويات الضوضاء. • تحسين كفاءة الطاقة: من خلال تقليل الاهتزاز، يمكن للجهاز المساعدة في تحسين كفاءة الطاقة في الآلات، مما يؤدي إلى جودة منتج أعلى وتقليل الخسائر. • انخفاض تكاليف الصيانة: من خلال تقليل البلى على الآلات، يمكن أن يساعد الجهاز في تقليل تكاليف الصيانة. • تعدد الاستخدامات: يمكن تكييف الجهاز مع مجموعة واسعة من الأجزاء والتطبيقات الميكانيكية.	• خدمة العملاء • الدعم التقني • التدريب • ملاحظات العملاء **القنوات** • المبيعات المباشرة: تباع مباشرة للمصنعين الصناعيين. • شركاء التوزيع • المبيعات عبر الإنترنت • الشراكات التقنية: التعاون مع الشركات الهندسية والاستشاريين لدمج الجهاز في تصميماتهم	• المصنعون الصناعيون: الشركات التي تصنع الآلات بأجزاء دوارة أو مهتزة، مثل مولدات الطاقة والمضخات. • شركات النفط والغاز: الشركات التي تشغل آبار وخطوط أنابيب النفط والغاز • شركات الطيران والدفاع: الشركات التي تصمم وتصنع الطائرات، والتي تتعرض للاهتزاز من المحركات والأجزاء المتحركة الأخرى • شركات تصنيع الأجهزة الطبية وشركات التي تعتمد على الدقة العالية.

هيكل التكلفة	إيرادات
• تكاليف التصنيع: تكاليف المواد الخام والعمالة والنفقات العامة المرتبطة بتصنيع الجهاز. • تكاليف التسويق والمبيعات: تكاليف تسويق وبيع الجهاز. • تكاليف دعم العملاء: تكاليف توفير الدعم التقني وخدمة العملاء للعملاء. • التكاليف العامة والإدارية: التكاليف العامة مثل المرتبات والإيجار والمرافق العامة.	• مبيعات الجهاز: الإيرادات الناتجة عن بيع الجهاز للعملاء. • رسوم الترخيص: الإيرادات الناتجة عن ترخيص التكنولوجيا لشركات أخرى. • عقود الصيانة: تقديم عقود صيانة لضمان الأداء الأمثل للجهاز. • التدريب والشهادة: فرض رسوم على برامج التدريب وإصدار الشهادات لموظفي العملاء. • خدمات تحليل البيانات: توفير خدمات تحليل البيانات للعملاء لمساعدتهم على تحسين أداء آلاتهم.

TechnoFoster

Contact Us

+213 46 25 61 33

incubator@univ-tiaret.dz

fb.com/techno.foster.incubator

Bibliography

[1] HASSANI Islem SAFI Abdelkader. “Etude théorique et modélisation des butées poreuses pour le contrôle des vibrations”. In: (June 2023).

[2] Faisal Rahmani, Jayanta Kumar Dutt, and R. Pandey. “Dynamic Characteristics of a Finite-Width Journal Bearing Lubricated with Powders”. In: Dec. 2015.

[3] Youyun Shang et al. “Design and Optimization of the Surface Texture at the Hydrostatic Bearing and the Spindle for High Precision Machining”. In: *Machines* 10 (Sept. 2022), p. 806. DOI: 10.3390/machines10090806.

[4] A. Bouzidane. *Conception d’un palier hydrostatique intelligent pour contrôler les vibrations de rotors*. Thèse de doctorat en génie. École de technologie supérieure, 2007. URL: https://books.google.dz/books?id=TtyE0AEACAAJ.

[5] SKF. URL: https://www.skf.com/au/products/rolling-bearings/ball-bearings/deep-groove-ball-bearings.

[6] James F. Lea and Lynn Rowlan. “12 - Electrical submersible pumps”. In: *Gas Well Deliquification (Third Edition)*. Ed. by James F. Lea and Lynn Rowlan. Third Edition. Gulf Drilling Guides. Gulf Professional Publishing, 2019, pp. 237–308. ISBN: 978-0-12-815897-5. DOI: https://doi.org/10.1016/B978-0-12-815897-5.00012-3. URL: https://www.sciencedirect.com/science/article/pii/B9780128158975000123.

[7] Benariba Aboubakeur. *Contribution à l’étude de la lubrification micropolaire : Applications aux paliers hydrostatiques*. 2018. URL: http://dspace.univ-tiaret.dz/handle/123456789/500.

[8] Qi Zhao et al. “Research Developments of Aerostatic Thrust Bearings: A Review”. In: *Applied Sciences* 12.23 (2022). ISSN: 2076-3417. DOI: 10.3390/app122311887. URL: https://www.mdpi.com/2076-3417/12/23/11887.

[9] Luis San Andrés. “Cryogenic Hybrid Fluid Film Bearings”. In: *Encyclopedia of Tribology*. Ed. by Q. Jane Wang and Yip-Wah Chung. Boston, MA: Springer US, 2013, pp. 630–641. ISBN: 978-0-387-92897-5. DOI: 10.1007/978-0-387-92897-5_55. URL: https://doi.org/10.1007/978-0-387-92897-5_55.

[10] Jianzhou Du et al. “Rational Design and Porosity of Porous Alumina Ceramic Membrane for Air Bearing”. In: *Membranes* 11.11 (2021). ISSN: 2077-0375. DOI: 10.3390/membranes11110872. URL: https://www.mdpi.com/2077-0375/11/11/872.

[11] Serguei Kunik. “Étude numérique et expérimentale du mécanisme de lubrification eX-Poro-HydroDynamique (XPHD)”. Thèse de doctorat dirigée par Fatu, Aurelian et Bouyer, Jean Mécanique des solides, des matériaux, des structures et des surfaces Poitiers 2018. PhD thesis. 2018. URL: http://www.theses.fr/2018POIT2264.

[12] Ammar MRABTI. “Lubrification par film comprimé de l’articulation fémoro-tibiale du genou humain”. In: (Sept. 2020).

[13] Jean-François Daïan. “Equilibre et transferts en milieux poreux”. In: 2013. URL: https://api.semanticscholar.org/CorpusID:102325478.

[14] Serguei Kunik. “Étude numérique et expérimentale du mécanisme de lubrification eX-Poro-HydroDynamique (XPHD)”. In: 2018. URL: https://api.semanticscholar.org/CorpusID:128242720.

[15] Xin Xiao et al. “Study on Static Characteristics of Aerostatic Bearing Based on Porous SiC Ceramic Membranes”. In: *Membranes* 12.9 (2022). ISSN: 2077-0375. DOI: 10.3390/membranes12090898. URL: https://www.mdpi.com/2077-0375/12/9/898.

Abstract

Aerostatic bearings provide a beneficial method for controlling rotor vibrations. This work focuses on investigating how the inherent permeability of porous aerostatic bearing can optimize the dynamic stability of rotores they support.

The study leverages a 3D computational fluid dynamics (CFD) using Ansys-CFX. The model is validated against established theoretical models and existing experimental data, suggesting the model's potential design principles for novel vibration control methods. The analysis revealed that distinct permeabilities within the porous material significantly influence the dynamic behavior of the bearing supporting a load. A novel approach to controlling rotary vibrations is offered by changing the positioning of cylindrical inserts, which allows for more precise rotational alignment and mitigates wear and tear.

Résumé

Les paliers aérostatiques fournissent une méthode bénéfique pour contrôler les vibrations du rotor. Ce travail se concentre sur l'étude de la façon dont la perméabilité inhérente des paliers aérostatiques poreux peut optimiser la stabilité dynamique des rotors qu'ils supportent.

L'étude s'appuie sur une dynamique des fluides computationnelle (CFD) 3D utilisant Ansys-CFX. Le modèle est validé par rapport aux modèles théoriques établis et aux données expérimentales existantes, ce qui suggère les principes de conception potentiels du modèle pour de nouvelles méthodes de contrôle des vibrations.

L'analyse a révélé que des perméabilités distinctes dans le matériau poreux influencent de manière significative le comportement dynamique du roulement supportant une charge. Une nouvelle approche pour contrôler les vibrations rotatives est proposée en modifiant le positionnement des inserts cylindriques, ce qui permet un alignement de rotation plus précis et atténue l'usure.

ملخص

توفر المحامل الهوائية طريقة مفيدة للتحكم في اهتزازات الدوار. تركز هذه الدراسة على كيفية تأثير النفاذية الذاتية للمحامل الهوائية المسامية على تحسين الاستقرار الديناميكي للدوارات التي تدعمها.
تعتمد الدراسة على ديناميكيات السوائل الرقمية (CFD) ثلاثية الأبعاد باستخدام برنامج $Ansys-CFX$. تم التحقق من صحة النموذج مقارنة بالنماذج النظرية السابقة والبيانات التجريبية الموجودة، مما يشير إلى صحة النموذج النظري .
كشفت التحليلات أن تباين النفاذيات في الوسط المسامي تؤثر بشكل كبير على السلوك الديناميكي للمحمل الذي يدعم الدوار. قمنا باقتراح نهج جديد للتحكم في الاهتزازات الدورانية عن طريق تعديل موضع القطع الأسطوانية المدرجة، مما يسمح بدوران أكثر دقة و انخفاض في التآكل.